Journal of Chemical&Engineering Data

pubs.acs.org/jced Article

# Density of *n*-Heptane + *n*-Dodecane and Carbon Dioxide + *n*-Heptane + *n*-Dodecane Mixtures up to 70 MPa from (293.15 to 363.15) K

David C. Santos, Isaque S. Gonçalves, Ana Mehl, Paulo Couto, and Márcio L. L. Paredes*

Cite This: *J. Chem. Eng. Data* 2021, 66, 1305−1318 Read Online

ACCESS | Metrics & More | Article Recommendations | Supporting Information

**ABSTRACT:** Density measurements of the *n*-heptane + *n*-dodecane binary mixture were performed with a vibrating tube densitometer in the temperature range of (293.15 to 363.15) K and pressure up to 70 MPa at six different *n*-heptane mole fractions: $x_1$ = 0, 0.1999, 0.3991, 0.5999, 0.7998, and 1. Densities of the $CO_2$ + *n*-heptane + *n*-dodecane ternary mixtures were also measured at the same temperature and pressure ranges for two different isopleths: $CO_2$ (0.4904) + *n*-heptane (0.2548) + *n*-dodecane (0.2548), and $CO_2$ (0.7425) + *n*-heptane (0.1288) + *n*-dodecane (0.1288). The obtained experimental data were correlated by a polynomial model and by a Tait-based equation. Density values for pure *n*-heptane and *n*-dodecane were found to be in agreement with literature data within approximately 0.3%. The isothermal compressibility and thermal expansion values of these mixtures were obtained by differentiation from the models as a function of pressure and temperature. Analysis of these properties pointed out that the polynomial model provided more accurate results related to derived properties. The excess volume of the mixtures was also determined. In general, they are negative, but they become positive for binary mixtures in the heptane-rich region as well as at higher pressures for ternary mixtures.

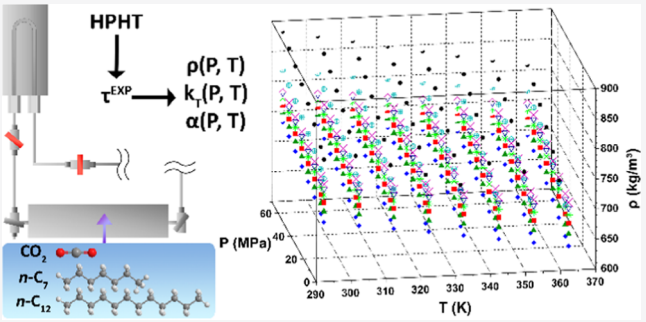


## 1. INTRODUCTION

The reduction in oil production from conventional sources has driven the global interest in the use of enhanced oil recovery methods (EOR). This fact led the oil and gas industry to explore formations characterized by more extreme production conditions than in conventional reservoirs. Carbon dioxide ($CO_2$) miscible flooding is among the most effective nonthermal EOR methods. In this method, $CO_2$ is injected through injection wells into the reservoir under high pressure causing a significant reduction in oil viscosity and swelling the oil.[1,2] Both oil swelling and viscosity reduction improve crude oil mobility, providing opportunities to recover oils that would not be produced. In this context, density measurements are important to characterize the thermodynamic volumetric properties and develop accurate equations of state for reservoir fluid description.

Due to the compositional complexity of crude oil, alkane mixtures under high pressure and high temperature (HPHT) were typically used as alternatives of crude oil to address the thermodynamic properties of crude oil. However, the amount of density data available in the literature covering the temperature and pressure conditions typically found in offshore reservoirs is still limited. For instance, a literature survey of studies of liquid densities for *n*-alkane binary mixtures reveals that only Dzida and Cempa[3] evaluated the *n*-heptane + *n*-dodecane system at HPHT. Their study reported the density of this mixture at temperatures from (293 to 318) K and pressure up to 100 MPa. Furthermore, the availability of density data for ternary or multicomponent mixtures comprising alkanes with dissolved $CO_2$ is even more restrictive.[4−7]

To understand the volumetric behavior of $CO_2$-rich fluids in oil reservoirs, both academia and industry have been using binary $CO_2$ + hydrocarbon mixtures as a model system. For instance, Fenghour et al.[4] measured the density of the $CO_2$ + *n*-heptane system from (405 to 469) K, for pressures between 0.7 and 24 MPa at the following carbon dioxide mole fractions: 0.2918, 0.3888, and 0.4270. Medina-Bermúdez et al.[8] extended this dataset for a temperate range of (313.15−363.15) K at pressures up to 25 MPa and $CO_2$ composition from 0.0218 to 0.9496. In addition, Bazile et al.[9] explored $CO_2$ + *n*-heptane mixture densities for a composition varying from 0.236 to

Received: October 28, 2020
Accepted: January 26, 2021
Published: February 3, 2021







https://dx.doi.org/10.1021/acs.jced.0c00943
J. Chem. Eng. Data 2021, 66, 1305−1318

0.869, at two temperatures near $CO_2$ critical temperature, $T$ = (303.15 and 313.15) K, and at pressures from 10 to 70 MPa.

The $CO_2$ + *n*-dodecane binary system has also been studied regarding volumetric behavior under HPHT conditions. Zhang et al.[10] studied the volumetric behavior of this mixture at four carbon dioxide mole fractions: 0.2497, 0.5094, 0.7576, and 0.8610, at temperatures ranging from (313.55 to 353.55) K, and pressure up to 18 MPa. Moreover, Zambrano et al.[11] also measured the experimental density data for the $CO_2$ + *n*-dodecane binary mixture at a temperature range of (283.15−393.15) K and $p$ = (10−100) MPa. Recently, Bazile et al.[12] measured densities of the $CO_2$ + *n*-dodecane mixture with $CO_2$ molar percentage ranging from 20 to 85% at pressures from (10 to 70) MPa and at two temperatures around the critical temperature of carbon dioxide (303 and 313) K. To the best of our knowledge, there are no available density data for the $CO_2$ + *n*-heptane + *n*-dodecane ternary system.

Thus, in this study, the density of pure *n*-heptane, *n*-dodecane, their binary mixtures, and the ternary mixture comprising *n*-heptane and *n*-dodecane with dissolved $CO_2$ were measured in a range of temperatures from (293.15 to 363.15) K and pressure up to 70 MPa.

Two models were used to correlate the density experimental data: an empirical polynomial model presented by Amorim et al.[13] and a Tait-based model. Amorim's equation calculates density data from other thermodynamic properties such as thermal expansion coefficient ($\alpha$) and isothermal compressibility coefficient ($k_T$). From this approach, the density of the cyclohexane + *n*-hexadecane binary mixtures from (318.15 to 413.15) K and up to 62 MPa presented deviations within the experimental error, which was notably more accurate than the simpler empirical models such as Tait-based models. Thus, this study also attempts to evaluate the Amorim and co-authors' equation[13] in systems that are significantly more compressible than the work previously evaluated by those authors.

## 2. MATERIALS AND METHODS

**2.1. Materials.** The pure *n*-heptane and *n*-dodecane used in this study were provided by Sigma-Aldrich with a stated mass fraction purity all higher than 0.99. Carbon dioxide was provided by White Martins with a stated mass fraction purity higher than 0.998. All reagents were used without further purification. The liquid hydrocarbons were degassed separately in vacuum flasks at least for 1 h by means of a VWR ultrasonic bath prior to their use. The details of the chemicals used in this work are listed in Table 1.

The *n*-heptane + *n*-dodecane binary mixtures are carefully prepared by the gravimetric method using a Mettler Toledo balance (ME204/A) with a combined standard uncertainty of 0.0002 g at six different *n*-heptane mole fractions: $x_1$ = 0, 0.1999, 0.3991, 0.5999, 0.7998, and 1. These substances were weighted one at a time in the same flask just before the measurement. The mixture was transferred to a high-pressure cylinder (sample cylinder) immediately after preparation to prevent evaporation. The cylinder is divided into two parts by means of an inner piston. One side of it was filled with water, which was used as a hydraulic fluid, whereas the other side was filled with the sample. The sample side was bled to remove trapped air from the cylinder. The estimated combined expand uncertainty, $U_c$, in the composition of the mixtures is $1 \times 10^{-5}$ in mole fraction with $k$ = 2 for a confidence level of 0.95,

For the preparation of the $CO_2$ + *n*-heptane + *n*-dodecane ternary mixture, an equimolar mixture of *n*-heptane + *n*-dodecane was first weighed in the sample cylinder using a Sartorius balance (Cubis MSU 10202S) with a combined standard uncertainty of 0.06 g. After that, the cylinder was closed to avoid evaporation and the sample side was bled to remove trapped air from the cylinder. Thus, a volumetric pump (Quizix Q5000) was used to inject the $CO_2$ (by sample side) in homogeneous liquid state within the measurement cell. The return line of the hydraulic fluid that connects the sample cylinder to an external vessel controlled the pressure in the system. Consequently, the mass of injected $CO_2$ into the measuring cell is directly determined by weighing the cylinder using mass balance principles. The composition and combined expand uncertainties in the composition of the ternary mixtures calculated by the uncertainty propagation law ($k$ = 2) are shown in Table 2.

**Table 1. Specifications of Chemicals in This Study[a]**

| chemical name | source | CAS registry number | mass fraction purity[a,b] | purification method |
|---|---|---|---|---|
| *n*-heptane | Sigma-Aldrich | 142-82-5 | >0.99 | none |
| *n*-dodecane | Sigma-Aldrich | 112-40-3 | >0.99 | none |
| carbon dioxide | White Martins | 124-38-9 | >0.998 | none |

[a]All of the purities of the samples were obtained by the suppliers, and no further purity measurements were performed. [b]Analysis performed by the supplier with gas chromatography.

**Table 2. Mole Fraction, $x$, and Combined Expand Uncertainties in the Composition, $U_c(x)$, of the Ternary Mixtures**

| substance | $x$ | $U_c(x)$ | $x$ | $U_c(x)$ |
|---|---|---|---|---|
| carbon dioxide | 0.4904 | $1.2 \times 10^{-3}$ | 0.7425 | $8.6 \times 10^{-4}$ |
| *n*-dodecane | 0.2548 | $7.3 \times 10^{-4}$ | 0.12875 | $5.0 \times 10^{-4}$ |
| *n*-heptane | 0.2548 | $9.0 \times 10^{-4}$ | 0.12875 | $7.6 \times 10^{-4}$ |

After the injection of $CO_2$ into the hydrocarbon mixture, the mixture is pressurized at 70 MPa and the cylinder was rocked for 24 h to generate the movement of a stainless steel ball placed inside the cylinder to achieve the homogenization of the prepared mixture.

**2.2. Density Measurements.** The density of the pure hydrocarbons and the mixtures was measured using a U-shaped vibrating tube densitometer Anton Paar DMA HPM, with an mPDS-5 evaluation unit as the reading device. In addition to the densitometer, the experimental setup includes one volumetric pump (Quizix Q5000) required to impose pressure within the measurement cell and a pressure transducer (AST 4300), which measures pressures up to 138 MPa with a standard uncertainty of 0.35 MPa. The measuring cell of the densitometer is maintained at a constant temperature through a liquid circulator bath Julabo 300F. The temperature is measured by a built-in temperature sensor. According to the manufacturer's specification, the temperature error is less than 0.1 K, and according to our measurements, the standard uncertainty $u(T)$ is 0.02 K. A schematic of the experimental apparatus can be found in Figure 1. Four times the volume of the tubes from the sample cylinder to the purging of the densitometer is expelled to ensure that the sample composition in the densitometer measuring cell is the same as that prepared in the sample cylinder.



https://dx.doi.org/10.1021/acs.jced.0c00943
J. Chem. Eng. Data 2021, 66, 1305−1318

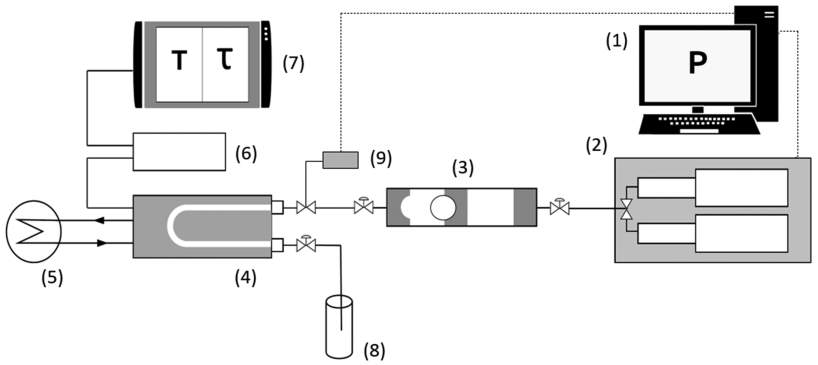


**Figure 1.** Schematic of the densitometer. (1) Computer, (2) Quizix Q5000 pumps, (3) sample cylinder, (4) DMA HPM, (5) Julabo 300F thermostatic bath, (6) HPM DMA interface module, (7) mPDS-5, (8) external sample receiver, and (9) pressure transducer.

The calibration of the densitometer was performed following a modification of the method presented in Lagourette et al.,[14] analogously to that described by Comuñas et al.[15] using vacuum and Milli-Q water as references. The mPDS-5 evaluation unit displays the oscillating period with seven digits, which, according to Comuñas et al.[15] and our experiments, corresponds to an uncertainty of the order of $10^{-2}$ kg·m$^{-3}$ related only to the measured oscillating period. Thus, considering the uncertainties of the temperature, the pressure, the period of oscillation measurements for water, vacuum, and the studied liquid, and density accuracy of the water density data,[16] the combined experimental uncertainty in the reported density values, by applying the law of propagating errors, is estimated to be 0.1 kg·m$^{-3}$. Fluid viscosity can also affect the vibration of the U-tube. For viscous fluids of about 150 mPa·s, density measurements can increase by about $\delta\rho = 0.0005{\cdot}\rho$.[17] In this work, the effect of viscosity on density measurements is considered negligible since the maximum viscosity of the evaluated systems is around 3 mPa·s.[18] Further analysis on sensitivity of vibrating U-tubes is reported by Holcomb and Outcalt.[19]

According to Chirico et al.,[20] for a sample of 99% mole fraction purity (*n*-heptane and *n*-dodecane; see Table 1), contribution of sample impurity to the combined standard uncertainty would be $u_c(\rho) = 0.001{\cdot}\rho$. Thus, considering propagation error law, the combined expanded uncertainty $U_c$ ($k = 2$ for a confidence level of 0.95) for density measurements of all systems evaluated in this study is $U_c(\rho) = 0.002{\cdot}\rho$.

Density measurements were performed in the temperature range from (293.15 to 363.15) K and pressures from (5 to 70) MPa for the *n*-heptane, *n*-dodecane, and their binary mixtures. The $CO_2$ + *n*-heptane + *n*-dodecane ternary mixtures are also studied in the aforementioned range of temperature and pressure. However, the minimum pressures of the measurements for ternary mixtures are set to values higher than their bubble pressures, which in turn were roughly calculated using commercial modeling software with the Peng−Robinson equation of state (EoS).[21]

**2.3. Modeling of Density and Calculation of Thermal Expansion Coefficient and Isothermal Compressibility Coefficient.** *2.3.1. Empirical Polynomial Model from α and $k_T$ (Polynomial).* A polynomial model for thermal expansion coefficient ($\alpha$, eq 1) and isothermal compressibility coefficient ($k_T$, eq 2) was used as presented by Amorim et al.[13] The density model is obtained after the integration of eq 1 at a reference pressure $p^*$ from a given temperature range ($T^*$ to $T$). Density value at reference $T^*$ and $p^*$ must be known. In the present study, these values were obtained experimentally. The final step is to integrate eq 2 from $p^*$ to a pressure $p$.

$$\alpha(T, p^*) = -\left[\frac{\partial \ln(\rho)}{\partial T}\right]_p \tag{1}$$

$$k_T(T, p) = \left[\frac{\partial \ln(\rho)}{\partial p}\right]_T \tag{2}$$

In this study, eqs 1 and 2 were used to obtain numerical $\alpha$ and $k_T$. To calculate numerical $\alpha$, the natural logarithm of experimental density at constant pressure was fitted by a polynomial equation relating density to the temperature. To calculate numerical $k_T$, the natural logarithm of experimental density at constant temperature was fitted by a polynomial equation relating density to the pressure.

From Amorim's proposal, $\alpha$ and $k_T$ are defined according to eqs 3 and 4.

$$\alpha(T, p^*) = a' + b'T + c'T^2 \tag{3}$$

$$k_T(T, p) = a(p) + b(p)T + c(p)T^2 \tag{4}$$

where

$$a(p) = a_0^P + a_1^P p + a_2^P p^2 \tag{5}$$

$$b(p) = b_0^P + b_1^P p + b_2^P p^2 \tag{6}$$

$$c(p) = c_0^P + c_1^P p + c_2^P p^2 \tag{7}$$

From basic thermodynamics

$$d\rho = \left(\frac{\partial \rho}{\partial p}\right)_T dp + \left(\frac{\partial \rho}{\partial T}\right)_p dT \tag{8}$$

$$\frac{d\rho}{\rho} = k_T dp - \alpha dT \tag{9}$$

Integrating term by term eq 9 to density, pressure, and temperature, respectively, and rearranging, density can be calculated as follows

$$\rho(p, T) = \rho^* \cdot e^{\int_{p^*}^{p} k_T dp' - \int_{T^*}^{T} \alpha dT'} \tag{10}$$

where $\rho^*$ is the density value at reference $T^*$ and $p^*$

Thus, integrating eqs 3 and 4, the densities can be calculated as a function of pressure and temperature with eq 10.



https://dx.doi.org/10.1021/acs.jced.0c00943
J. Chem. Eng. Data 2021, 66, 1305−1318

Table 3. Experimental Densities $\rho$ for *n*-Heptane (1) + *n*-Dodecane at Temperature $T$, Pressure $p$, and Mole Fraction $x_1$[a]

| $p$/MPa | $T$/K | $x_1$ | $\rho$/kg·m$^{-3}$ | $T$/K | $x_1$ | $\rho$/kg·m$^{-3}$ |
|---|---|---|---|---|---|---|
| 5 | 293.15 | 0.0000 | 752.3 | 303.15 | 0.0000 | 745.3 |
| 5 | 293.15 | 0.1999 | 743.6 | 303.15 | 0.1999 | 736.6 |
| 5 | 293.15 | 0.3991 | 734.0 | 303.15 | 0.3991 | 726.6 |
| 5 | 293.15 | 0.5999 | 721.8 | 303.15 | 0.5999 | 714.3 |
| 5 | 293.15 | 0.7998 | 707.1 | 303.15 | 0.7998 | 699.3 |
| 5 | 293.15 | 1.0000 | 689.0 | 303.15 | 1.0000 | 680.7 |
| 10 | 293.15 | 0.0000 | 755.7 | 303.15 | 0.0000 | 748.8 |
| 10 | 293.15 | 0.1999 | 747.2 | 303.15 | 0.1999 | 740.2 |
| 10 | 293.15 | 0.3991 | 737.6 | 303.15 | 0.3991 | 730.5 |
| 10 | 293.15 | 0.5999 | 725.5 | 303.15 | 0.5999 | 718.4 |
| 10 | 293.15 | 0.7998 | 711.1 | 303.15 | 0.7998 | 703.6 |
| 10 | 293.15 | 1.0000 | 693.5 | 303.15 | 1.0000 | 685.3 |
| 20 | 293.15 | 0.0000 | 761.9 | 303.15 | 0.0000 | 755.3 |
| 20 | 293.15 | 0.1999 | 753.7 | 303.15 | 0.1999 | 747.1 |
| 20 | 293.15 | 0.3991 | 744.3 | 303.15 | 0.3991 | 737.5 |
| 20 | 293.15 | 0.5999 | 732.5 | 303.15 | 0.5999 | 725.6 |
| 20 | 293.15 | 0.7998 | 718.5 | 303.15 | 0.7998 | 711.3 |
| 20 | 293.15 | 1.0000 | 701.3 | 303.15 | 1.0000 | 693.7 |
| 30 | 293.15 | 0.0000 | 767.6 | 303.15 | 0.0000 | 761.3 |
| 30 | 293.15 | 0.1999 | 759.5 | 303.15 | 0.1999 | 753.2 |
| 30 | 293.15 | 0.3991 | 750.4 | 303.15 | 0.3991 | 743.9 |
| 30 | 293.15 | 0.5999 | 738.8 | 303.15 | 0.5999 | 732.4 |
| 30 | 293.15 | 0.7998 | 725.2 | 303.15 | 0.7998 | 718.4 |
| 30 | 293.15 | 1.0000 | 708.4 | 303.15 | 1.0000 | 701.2 |
| 40 | 293.15 | 0.0000 | 773.0 | 303.15 | 0.0000 | 767.0 |
| 40 | 293.15 | 0.1999 | 765.0 | 303.15 | 0.1999 | 759.0 |
| 40 | 293.15 | 0.3991 | 756.1 | 303.15 | 0.3991 | 749.9 |
| 40 | 293.15 | 0.5999 | 744.9 | 303.15 | 0.5999 | 738.6 |
| 40 | 293.15 | 0.7998 | 731.5 | 303.15 | 0.7998 | 724.9 |
| 40 | 293.15 | 1.0000 | 715.0 | 303.15 | 1.0000 | 708.1 |
| 50 | 293.15 | 0.0000 | 778.1 | 303.15 | 0.0000 | 772.2 |
| 50 | 293.15 | 0.1999 | 770.3 | 303.15 | 0.1999 | 764.4 |
| 50 | 293.15 | 0.3991 | 761.4 | 303.15 | 0.3991 | 755.4 |
| 50 | 293.15 | 0.5999 | 750.4 | 303.15 | 0.5999 | 744.2 |
| 50 | 293.15 | 0.7998 | 737.1 | 303.15 | 0.7998 | 730.9 |
| 50 | 293.15 | 1.0000 | 721.0 | 303.15 | 1.0000 | 714.4 |
| 60 | 293.15 | 0.0000 | 782.7 | 303.15 | 0.0000 | 777.2 |
| 60 | 293.15 | 0.1999 | 775.1 | 303.15 | 0.1999 | 769.4 |
| 60 | 293.15 | 0.3991 | 766.4 | 303.15 | 0.3991 | 760.7 |
| 60 | 293.15 | 0.5999 | 755.5 | 303.15 | 0.5999 | 749.6 |
| 60 | 293.15 | 0.7998 | 742.5 | 303.15 | 0.7998 | 736.4 |
| 60 | 293.15 | 1.0000 | 726.7 | 303.15 | 1.0000 | 720.2 |
| 70 | 293.15 | 0.0000 | 787.4 | 303.15 | 0.0000 | 781.8 |
| 70 | 293.15 | 0.1999 | 779.8 | 303.15 | 0.1999 | 774.2 |
| 70 | 293.15 | 0.3991 | 771.3 | 303.15 | 0.3991 | 765.7 |
| 70 | 293.15 | 0.5999 | 760.5 | 303.15 | 0.5999 | 754.7 |
| 70 | 293.15 | 0.7998 | 747.6 | 303.15 | 0.7998 | 741.7 |
| 70 | 293.15 | 1.0000 | 732.0 | 303.15 | 1.0000 | 726.0 |
| 5 | 313.15 | 0.0000 | 738.2 | 323.15 | 0.0000 | 731.6 |
| 5 | 313.15 | 0.1999 | 729.3 | 323.15 | 0.1999 | 722.2 |
| 5 | 313.15 | 0.3991 | 719.5 | 323.15 | 0.3991 | 712.4 |
| 5 | 313.15 | 0.5999 | 706.4 | 323.15 | 0.5999 | 699.3 |
| 5 | 313.15 | 0.7998 | 691.3 | 323.15 | 0.7998 | 683.8 |
| 5 | 313.15 | 1.0000 | 672.8 | 323.15 | 1.0000 | 664.9 |
| 10 | 313.15 | 0.0000 | 741.9 | 323.15 | 0.0000 | 735.0 |
| 10 | 313.15 | 0.1999 | 733.1 | 323.15 | 0.1999 | 725.9 |
| 10 | 313.15 | 0.3991 | 723.4 | 323.15 | 0.3991 | 716.1 |
| 10 | 313.15 | 0.5999 | 710.6 | 323.15 | 0.5999 | 703.4 |
| 10 | 313.15 | 0.7998 | 695.9 | 323.15 | 0.7998 | 688.2 |
| 10 | 313.15 | 1.0000 | 677.7 | 323.15 | 1.0000 | 669.6 |
| 20 | 313.15 | 0.0000 | 748.8 | 323.15 | 0.0000 | 742.3 |
| 20 | 313.15 | 0.1999 | 740.2 | 323.15 | 0.1999 | 733.9 |
| 20 | 313.15 | 0.3991 | 730.8 | 323.15 | 0.3991 | 724.0 |
| 20 | 313.15 | 0.5999 | 718.5 | 323.15 | 0.5999 | 711.6 |
| 20 | 313.15 | 0.7998 | 704.1 | 323.15 | 0.7998 | 696.9 |
| 20 | 313.15 | 1.0000 | 685.9 | 323.15 | 1.0000 | 679.2 |
| 30 | 313.15 | 0.0000 | 755.2 | 323.15 | 0.0000 | 748.9 |
| 30 | 313.15 | 0.1999 | 746.9 | 323.15 | 0.1999 | 740.7 |
| 30 | 313.15 | 0.3991 | 737.6 | 323.15 | 0.3991 | 731.1 |
| 30 | 313.15 | 0.5999 | 725.5 | 323.15 | 0.5999 | 718.9 |
| 30 | 313.15 | 0.7998 | 711.7 | 323.15 | 0.7998 | 704.8 |
| 30 | 313.15 | 1.0000 | 694.7 | 323.15 | 1.0000 | 687.5 |
| 40 | 313.15 | 0.0000 | 761.0 | 323.15 | 0.0000 | 755.0 |
| 40 | 313.15 | 0.1999 | 752.7 | 323.15 | 0.1999 | 747.0 |
| 40 | 313.15 | 0.3991 | 743.7 | 323.15 | 0.3991 | 737.7 |
| 40 | 313.15 | 0.5999 | 732.0 | 323.15 | 0.5999 | 725.7 |
| 40 | 313.15 | 0.7998 | 718.4 | 323.15 | 0.7998 | 711.8 |
| 40 | 313.15 | 1.0000 | 701.7 | 323.15 | 1.0000 | 695.0 |
| 50 | 313.15 | 0.0000 | 766.4 | 323.15 | 0.0000 | 760.7 |
| 50 | 313.15 | 0.1999 | 758.3 | 323.15 | 0.1999 | 752.9 |
| 50 | 313.15 | 0.3991 | 749.6 | 323.15 | 0.3991 | 743.7 |
| 50 | 313.15 | 0.5999 | 738.0 | 323.15 | 0.5999 | 732.0 |
| 50 | 313.15 | 0.7998 | 724.6 | 323.15 | 0.7998 | 718.5 |
| 50 | 313.15 | 1.0000 | 708.3 | 323.15 | 1.0000 | 702.0 |
| 60 | 313.15 | 0.0000 | 771.5 | 323.15 | 0.0000 | 766.1 |
| 60 | 313.15 | 0.1999 | 763.7 | 323.15 | 0.1999 | 758.4 |
| 60 | 313.15 | 0.3991 | 754.9 | 323.15 | 0.3991 | 749.3 |
| 60 | 313.15 | 0.5999 | 743.5 | 323.15 | 0.5999 | 737.8 |
| 60 | 313.15 | 0.7998 | 730.4 | 323.15 | 0.7998 | 724.5 |
| 60 | 313.15 | 1.0000 | 714.3 | 323.15 | 1.0000 | 708.4 |
| 70 | 313.15 | 0.0000 | 776.3 | 323.15 | 0.0000 | 771.0 |
| 70 | 313.15 | 0.1999 | 768.5 | 323.15 | 0.1999 | 763.4 |
| 70 | 313.15 | 0.3991 | 760.0 | 323.15 | 0.3991 | 754.5 |
| 70 | 313.15 | 0.5999 | 748.8 | 323.15 | 0.5999 | 743.1 |
| 70 | 313.15 | 0.7998 | 735.9 | 323.15 | 0.7998 | 730.1 |
| 70 | 313.15 | 1.0000 | 720.1 | 323.15 | 1.0000 | 714.3 |
| 5 | 333.15 | 0.0000 | 724.1 | 343.15 | 0.0000 | 717.1 |
| 5 | 333.15 | 0.1999 | 715.2 | 343.15 | 0.1999 | 707.6 |
| 5 | 333.15 | 0.3991 | 704.7 | 343.15 | 0.3991 | 697.3 |
| 5 | 333.15 | 0.5999 | 691.5 | 343.15 | 0.5999 | 683.8 |
| 5 | 333.15 | 0.7998 | 675.4 | 343.15 | 0.7998 | 667.5 |
| 5 | 333.15 | 1.0000 | 656.1 | 343.15 | 1.0000 | 647.6 |
| 10 | 333.15 | 0.0000 | 728.2 | 343.15 | 0.0000 | 721.4 |
| 10 | 333.15 | 0.1999 | 719.5 | 343.15 | 0.1999 | 712.4 |
| 10 | 333.15 | 0.3991 | 709.1 | 343.15 | 0.3991 | 702.0 |
| 10 | 333.15 | 0.5999 | 696.2 | 343.15 | 0.5999 | 688.8 |
| 10 | 333.15 | 0.7998 | 680.5 | 343.15 | 0.7998 | 672.9 |
| 10 | 333.15 | 1.0000 | 661.6 | 343.15 | 1.0000 | 653.6 |
| 20 | 333.15 | 0.0000 | 735.8 | 343.15 | 0.0000 | 729.4 |
| 20 | 333.15 | 0.1999 | 727.3 | 343.15 | 0.1999 | 720.5 |
| 20 | 333.15 | 0.3991 | 717.4 | 343.15 | 0.3991 | 710.7 |
| 20 | 333.15 | 0.5999 | 704.9 | 343.15 | 0.5999 | 698.0 |
| 20 | 333.15 | 0.7998 | 689.8 | 343.15 | 0.7998 | 682.7 |
| 20 | 333.15 | 1.0000 | 671.7 | 343.15 | 1.0000 | 664.3 |
| 30 | 333.15 | 0.0000 | 742.7 | 343.15 | 0.0000 | 736.2 |
| 30 | 333.15 | 0.1999 | 734.4 | 343.15 | 0.1999 | 728.1 |
| 30 | 333.15 | 0.3991 | 724.8 | 343.15 | 0.3991 | 718.4 |
| 30 | 333.15 | 0.5999 | 712.5 | 343.15 | 0.5999 | 706.1 |
| 30 | 333.15 | 0.7998 | 698.0 | 343.15 | 0.7998 | 691.4 |
| 30 | 333.15 | 1.0000 | 680.6 | 343.15 | 1.0000 | 673.6 |
| 40 | 333.15 | 0.0000 | 749.1 | 343.15 | 0.0000 | 743.3 |
| 40 | 333.15 | 0.1999 | 741.1 | 343.15 | 0.1999 | 735.0 |



https://dx.doi.org/10.1021/acs.jced.0c00943
J. Chem. Eng. Data 2021, 66, 1305−1318

**Table 3. continued**

| $p$/MPa | $T$/K | $x_1$ | $\rho$/kg·m$^{-3}$ | $T$/K | $x_1$ | $\rho$/kg·m$^{-3}$ |
|---|---|---|---|---|---|---|
| 40 | 333.15 | 0.3991 | 731.7 | 343.15 | 0.3991 | 725.6 |
| 40 | 333.15 | 0.5999 | 719.7 | 343.15 | 0.5999 | 713.6 |
| 40 | 333.15 | 0.7998 | 705.5 | 343.15 | 0.7998 | 699.2 |
| 40 | 333.15 | 1.0000 | 688.4 | 343.15 | 1.0000 | 681.8 |
| 50 | 333.15 | 0.0000 | 754.9 | 343.15 | 0.0000 | 749.4 |
| 50 | 333.15 | 0.1999 | 747.1 | 343.15 | 0.1999 | 741.3 |
| 50 | 333.15 | 0.3991 | 737.9 | 343.15 | 0.3991 | 732.1 |
| 50 | 333.15 | 0.5999 | 726.1 | 343.15 | 0.5999 | 720.3 |
| 50 | 333.15 | 0.7998 | 712.3 | 343.15 | 0.7998 | 706.2 |
| 50 | 333.15 | 1.0000 | 695.5 | 343.15 | 1.0000 | 689.3 |
| 60 | 333.15 | 0.0000 | 760.3 | 343.15 | 0.0000 | 755.0 |
| 60 | 333.15 | 0.1999 | 752.7 | 343.15 | 0.1999 | 747.0 |
| 60 | 333.15 | 0.3991 | 743.6 | 343.15 | 0.3991 | 738.0 |
| 60 | 333.15 | 0.5999 | 732.1 | 343.15 | 0.5999 | 726.5 |
| 60 | 333.15 | 0.7998 | 718.4 | 343.15 | 0.7998 | 712.7 |
| 60 | 333.15 | 1.0000 | 702.0 | 343.15 | 1.0000 | 696.1 |
| 70 | 333.15 | 0.0000 | 765.4 | 343.15 | 0.0000 | 760.6 |
| 70 | 333.15 | 0.1999 | 757.8 | 343.15 | 0.1999 | 752.7 |
| 70 | 333.15 | 0.3991 | 749.0 | 343.15 | 0.3991 | 743.9 |
| 70 | 333.15 | 0.5999 | 737.6 | 343.15 | 0.5999 | 732.5 |
| 70 | 333.15 | 0.7998 | 724.1 | 343.15 | 0.7998 | 719.0 |
| 70 | 333.15 | 1.0000 | 708.2 | 343.15 | 1.0000 | 702.8 |
| 5 | 353.15 | 0.0000 | 709.9 | 363.15 | 0.0000 | 703.0 |
| 5 | 353.15 | 0.1999 | 700.3 | 363.15 | 0.1999 | 693.6 |
| 5 | 353.15 | 0.3991 | 689.7 | 363.15 | 0.3991 | 682.5 |
| 5 | 353.15 | 0.5999 | 675.9 | 363.15 | 0.5999 | 668.3 |
| 5 | 353.15 | 0.7998 | 659.4 | 363.15 | 0.7998 | 651.2 |
| 5 | 353.15 | 1.0000 | 638.8 | 363.15 | 1.0000 | 630.2 |
| 10 | 353.15 | 0.0000 | 714.6 | 363.15 | 0.0000 | 707.7 |
| 10 | 353.15 | 0.1999 | 705.4 | 363.15 | 0.1999 | 698.4 |
| 10 | 353.15 | 0.3991 | 694.6 | 363.15 | 0.3991 | 687.6 |
| 10 | 353.15 | 0.5999 | 681.2 | 363.15 | 0.5999 | 673.9 |
| 10 | 353.15 | 0.7998 | 665.2 | 363.15 | 0.7998 | 657.3 |
| 10 | 353.15 | 1.0000 | 645.4 | 363.15 | 1.0000 | 637.1 |
| 20 | 353.15 | 0.0000 | 723.1 | 363.15 | 0.0000 | 716.4 |
| 20 | 353.15 | 0.1999 | 714.2 | 363.15 | 0.1999 | 707.6 |
| 20 | 353.15 | 0.3991 | 703.7 | 363.15 | 0.3991 | 697.3 |
| 20 | 353.15 | 0.5999 | 691.2 | 363.15 | 0.5999 | 684.1 |
| 20 | 353.15 | 0.7998 | 675.7 | 363.15 | 0.7998 | 668.3 |
| 20 | 353.15 | 1.0000 | 656.8 | 363.15 | 1.0000 | 649.1 |
| 30 | 353.15 | 0.0000 | 730.6 | 363.15 | 0.0000 | 724.2 |
| 30 | 353.15 | 0.1999 | 721.8 | 363.15 | 0.1999 | 715.7 |
| 30 | 353.15 | 0.3991 | 711.8 | 363.15 | 0.3991 | 705.6 |
| 30 | 353.15 | 0.5999 | 699.6 | 363.15 | 0.5999 | 693.0 |
| 30 | 353.15 | 0.7998 | 684.8 | 363.15 | 0.7998 | 677.9 |
| 30 | 353.15 | 1.0000 | 666.6 | 363.15 | 1.0000 | 659.4 |
| 40 | 353.15 | 0.0000 | 737.4 | 363.15 | 0.0000 | 731.5 |
| 40 | 353.15 | 0.1999 | 729.1 | 363.15 | 0.1999 | 723.1 |
| 40 | 353.15 | 0.3991 | 719.3 | 363.15 | 0.3991 | 713.4 |
| 40 | 353.15 | 0.5999 | 707.3 | 363.15 | 0.5999 | 701.1 |
| 40 | 353.15 | 0.7998 | 692.8 | 363.15 | 0.7998 | 686.3 |
| 40 | 353.15 | 1.0000 | 675.3 | 363.15 | 1.0000 | 668.6 |
| 50 | 353.15 | 0.0000 | 743.7 | 363.15 | 0.0000 | 738.1 |
| 50 | 353.15 | 0.1999 | 735.6 | 363.15 | 0.1999 | 729.9 |
| 50 | 353.15 | 0.3991 | 726.0 | 363.15 | 0.3991 | 720.5 |
| 50 | 353.15 | 0.5999 | 714.3 | 363.15 | 0.5999 | 708.3 |
| 50 | 353.15 | 0.7998 | 700.2 | 363.15 | 0.7998 | 694.0 |
| 50 | 353.15 | 1.0000 | 683.1 | 363.15 | 1.0000 | 676.8 |
| 60 | 353.15 | 0.0000 | 749.6 | 363.15 | 0.0000 | 744.1 |
| 60 | 353.15 | 0.1999 | 741.8 | 363.15 | 0.1999 | 736.1 |
| 60 | 353.15 | 0.3991 | 732.3 | 363.15 | 0.3991 | 726.8 |
| 60 | 353.15 | 0.5999 | 720.7 | 363.15 | 0.5999 | 714.9 |
| 60 | 353.15 | 0.7998 | 706.9 | 363.15 | 0.7998 | 701.0 |
| 60 | 353.15 | 1.0000 | 690.2 | 363.15 | 1.0000 | 684.1 |
| 70 | 353.15 | 0.0000 | 755.2 | 363.15 | 0.0000 | 750.0 |
| 70 | 353.15 | 0.1999 | 747.5 | 363.15 | 0.1999 | 742.2 |
| 70 | 353.15 | 0.3991 | 738.1 | 363.15 | 0.3991 | 733.1 |
| 70 | 353.15 | 0.5999 | 726.8 | 363.15 | 0.5999 | 721.4 |
| 70 | 353.15 | 0.7998 | 713.3 | 363.15 | 0.7998 | 707.7 |
| 70 | 353.15 | 1.0000 | 696.8 | 363.15 | 1.0000 | 691.1 |

[a]Standard uncertainties are $U_c(x_1) = 1 \times 10^{-5}$, $u(T) = 0.02$ K, $u(p) = 0.35$ MPa. The combined expanded uncertainty is $U_c(\rho) = 0.002 \cdot \rho$ with 0.95 level of confidence ($k = 2$).

The Nelder–Mead simplex method[22] was used to fit the values of the fitting parameters found in eqs 3–7 to minimize the objective function ($F_{obj}$), given by the following equation

$$F_{obj} = \sqrt{\frac{\sum_{i=1}^{N} (\rho_i^{exp} - \rho_i^{calc})^2}{N}} \tag{11}$$

where $\rho^{exp}$ is the value of the experimental property determined in this work, $\rho^{calc}$ is the calculated value of the same property, and $N$ is the number of experimental data points.

*2.3.2. Tait Empirical Model (Tait).* The experimental densities were also correlated for each of the studied systems by means of the following modified Tammann–Tait equation[23]

$$\rho(T, p) = \frac{\rho(T, p_{ref})}{1 - C \ln\left(\frac{B(T) + p}{B(T) + p_{ref}}\right)} \tag{12}$$

where $\rho(T, p_{ref})$ is the density as a function of temperature at a reference pressure, given by the following equation

$$\rho(T, p_{ref}) = \sum_{i=0}^{m} A_i T^i \tag{13}$$

where $C$ is a constant and $B(T)$ is a temperature-dependent parameter given by

$$B(T) = \sum_{j=0}^{n} B_j T^j \tag{14}$$

where $A_i$, $B_j$, and $C$ are fitting parameters determined by correlating simultaneously for each composition the experimental densities values versus pressure and temperature.

The fitting parameters of eqs 13 and 14 were also optimized using eq 11.

The thermal expansion coefficient and the isothermal compressibility coefficient of the systems were also calculated using the Tait-based model. These derived thermodynamic properties were calculated by differentiation of eq 12, according to eqs 15 and 16.



https://dx.doi.org/10.1021/acs.jced.0c00943
J. Chem. Eng. Data 2021, 66, 1305–1318

Table 4. Summary of Density Data of *n*-Heptane, *n*-Dodecane, and *n*-Heptane + *n*-Dodecane Binary Mixture[a]

| year | author | $N_p$ | purity % | method | $T$/K | $p$/MPa |
|---|---|---|---|---|---|---|
| | | | *n*-heptane | | | |
| 2013 | Sagdeev et al.[24] | 48 | 99.99 | hw[b] | 298−470 | 0.1−245 |
| 2015 | Guerrero et al.[25] | 100 | 99 | vb[c] | 283−323 | 0.1−65 |
| 2016 | Abdussalam et al.[26] | 208 | 99 | vb | 288−413 | 0.1−60 |
| 2018 | Bazile et al.[9] | 14 | 99.5 | vb | 303−313 | 10−70 |
| | | | *n*-dodecane | | | |
| 1980 | Landau and Würflinger[27] | 226 | | vc[d] | 252−313 | 0.1−300 |
| 1981 | Dymond et al.[28] | 28 | 99 | vc | 298−373 | 0.1−502 |
| 2003 | Khasanshin et al.[29] | 104 | | sv[e] | 293−433 | 0.1−140 |
| 2007 | Elizalde-Solis et al.[30] | 150 | 99 | vb | 313−362 | 1−25 |
| 2008 | Dzida and Cempa[3] | 60 | 99 | sv | 293−318 | 0.1−100 |
| 2009 | Valencia et al.[31] | 54 | 99 | vb | 283−323 | 0.1−60 |
| 2014 | Zhang et al.[10] | 38 | 99 | msb[f] | 314−354 | 8−18 |
| 2015 | Regueira et al.[32] | 63 | 99.8 | vb | 278−463 | 0.1−60 |
| 2017 | García-Morales et al.[33] | 66 | 99.6 | vb | 293−393 | 0.1−70 |
| 2018 | Jia et al.[34] | 108 | 99 | vb | 283−362 | 0.1−100 |
| 2019 | Bazile et al.[12] | 14 | 99.6 | vb | 303−313 | 10−70 |
| | | | *n*-heptane + *n*-dodecane | | | |
| 2008 | Dzida and Cempa[3] | 480 | 99 | sv | 293−318 | 0.1−100 |

[a]The overall number of data points, $N_p$; temperature, $T$, and pressure, $p$, ranges; experimental method used; and purities of measured samples. [b]hw, hydrostatic weighing. [c]vb, vibrating tube. [d]vc, volume change. [e]sv, sound velocity. [f]msb, magnetic suspension balance.

$$k_T(T, p) = \frac{1}{\rho}\left(\frac{\partial \rho}{\partial p}\right)_T \equiv \frac{C}{[B(T) + p]\left[1 - C \ln\left(\frac{B(T) + p}{B(T) + p_{ref}}\right)\right]} \quad (15)$$

$$\alpha(T, p) = -\frac{1}{\rho}\left(\frac{\partial \rho}{\partial T}\right)_p \equiv -\frac{1}{\rho}\left(\frac{\rho'_0(T)D(T, p) - \rho_0(T)D'(T, p)}{D(T, p)^2}\right) \quad (16)$$

where $D(T,p)$ is the denominator of the Tait equation (eq 12) and $D'(T,p)$ is its temperature derivative defined as follows

$$D'(T, p) = \left(\frac{\partial D(T, p)}{\partial T}\right)_p \equiv CB'(T)\left(\frac{1}{B(T) + 0.1} - \frac{1}{B(T) + p}\right) \quad (17)$$

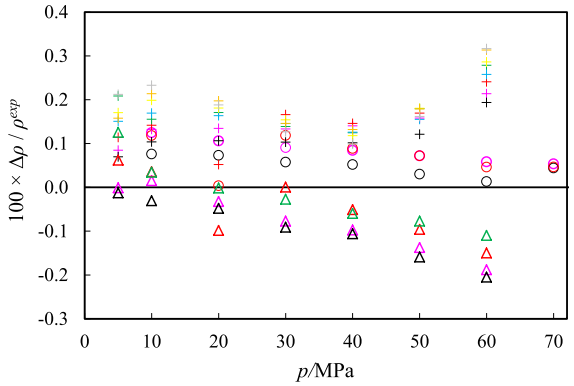


**Figure 2.** Fractional deviations $\Delta\rho = \rho^{exp} - \rho^{lit}$ of the experimental densities $\rho^{exp}$ of pure *n*-heptane from the values of $\rho^{lit}$ obtained from experimental data available in the literature as a function of pressure. (○) Dzida and Cempa,[3] (Δ) Guerrero et al.,[25] and (+) Abdussalam et al.[26] $T$ = 293.15 (pink), $T$ = 303.15 K (black), $T$ = 313.15 K (red), $T$ = 323.15 K (green), $T$ = 333.15 K (blue), $T$ = 343.15 K (yellow), $T$ = 353.15 K (orange), and $T$ = 363.15 K (gray).

## 3. RESULTS AND DISCUSSION

**3.1. Density.** The measurements were performed along eight isotherms, (293.15−363.15) K, for various pressures ranging from (5 to 70) MPa for pure *n*-heptane, *n*-dodecane, and four different binary mixtures of *n*-heptane + *n*-dodecane, ranging from (19.99 to 79.99) mol % of *n*-heptane. The measurements were also performed for the ternary mixture $CO_2$ (1) + *n*-heptane (2) + *n*-dodecane in two different $CO_2$ proportions: $x_1$ = 0.4904 and $x_1$ = 0.7525 at the same temperature and pressure range. For ternary systems, $x_2 = x_3$. The minimum pressures of the measurements were set to values higher than the saturation pressures. Thus, for the system with lower $CO_2$ content, the minimum pressure measurements are 5 MPa from (293.15 to 313.15) K and 10 MPa from (323.15 to 363.15) K. For the system with a higher $CO_2$ content, they are 5 MPa at 293.15 K, 10 MPa from (303.15 to 333.15) K, and 20 MPa from (343.15 to 363.15) K.

For comparing the experimental density values with those obtained with the correlations presented in Section 2.3, the absolute average deviation (AAD), the maximum deviation (MD), and the standard deviation ($\sigma$) are calculated and defined according to eqs 18−20.

$$\mathrm{AAD}/\% = \frac{100}{N}\sum_{i=1}^{N}\left|\frac{\rho_i^{exp} - \rho_i^{calc}}{\rho_i^{exp}}\right| \quad (18)$$

$$\mathrm{MD}/\% = \max\left(100\left|\frac{\rho_i^{exp} - \rho_i^{calc}}{\rho_i^{exp}}\right|\right) \quad (19)$$



https://dx.doi.org/10.1021/acs.jced.0c00943
J. Chem. Eng. Data 2021, 66, 1305−1318

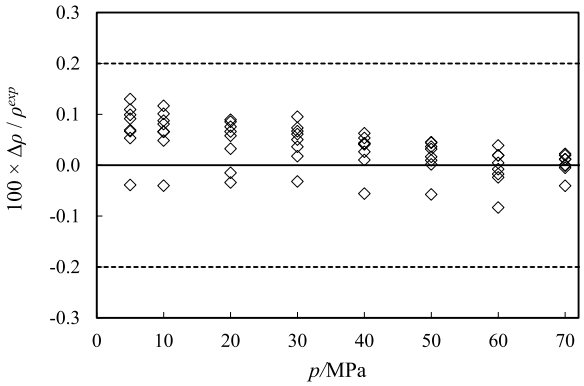


**Figure 3.** Fractional deviations $\Delta\rho = \rho^{exp} - \rho^{calc}$ of the experimental densities $\rho^{exp}$ of pure *n*-heptane at $T$ = (293.15−363.15) K from the values of $\rho^{calc}$ estimated from the correlation of Lemmon and Span[35] as a function of pressure. The dashed line is the combined expanded uncertainty $U_c(\rho) = 0.002*\rho$ with a confidence level of 0.95 ($k$ = 2).

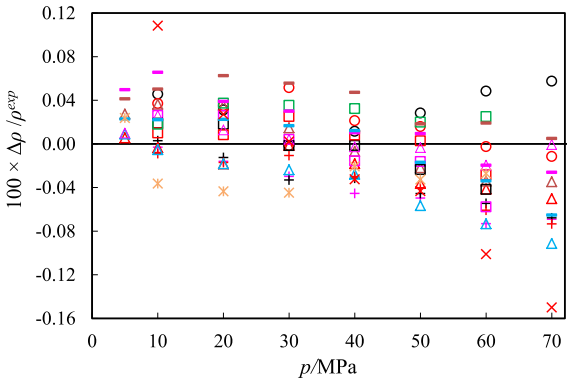


**Figure 4.** Fractional deviations $\Delta\rho = \rho^{exp} - \rho^{lit}$ of the experimental densities $\rho^{exp}$ of pure *n*-dodecane from the values of $\rho^{lit}$ obtained from the experimental data available in the literature as a function of pressure. (×) Landau and Würflinger,[27] (Δ) Khasanshin et al.,[29] (+) Dzida and Cempa,[3] (□) Valencia et al.,[31] (*) Regueira et al.,[32] (−) García-Morales et al.,[33] and (○) Bazile et al.[12] $T$ = 293.15 (pink), $T$ = 303.15 K (black), $T$ = 313.15 K (red), $T$ = 323.15 K (green), $T$ = 333.15 K (blue), and $T$ = 353.15 K (orange).

$$\sigma = \sqrt{\frac{\sum_{i=1}^{N} (\rho_i^{exp} - \rho_i^{calc})^2}{N - P}} \quad (20)$$

where $P$ is the number of fitting parameters.

*3.1.1. n-Heptane + n-Dodecane System.* The experimental densities of *n*-heptane, *n*-dodecane, and their binary mixtures are reported in Table 3. The literature density data of these substances are listed in Table 4. However, it is important to note that Table 4 only presents studies published after 2013 for *n*-heptane, and a previous study was conducted by Sagdeev et al.[24] who reported an extensive survey related to *n*-heptane density data.

Figure 2 shows the differences in density of the experimental values measured in this study and those found in recent works published in the literature for pure *n*-heptane. To evaluate all of our pure *n*-heptane density data, the experimental results were compared with the density calculated from the equation of state (EoS) developed by Lemmon and Span,[35] which presents the volumetric properties of *n*-heptane with high accuracy. Typical density uncertainties using this equation are 0.1−0.2%. Figure 3 shows the difference between the experimental data and those calculated from the EoS of Lemmon and Span.[35] The differences in density of the experimental values measured in this study and those found in the literature for *n*-dodecane are shown in Figure 4.

As can be seen in Figures 2−4, the deviations between the experimental densities and literature values (experimental and calculated) are mostly lower than 0.2%. More specifically, Figure 2 shows that data of the present study agree well with those reported by Dzida and Cempa[3] with deviations ranging from 0.004 to 0.12%. However, higher deviations can occur in comparison to the data reported by Guerrero et al.[25] and Abdussalam et al.,[26] reaching 0.20 and 0.32%, respectively. Furthermore, in Figure 2, it is also possible to note that the deviations between data of this study and those of Guerrero et al.[25] and Abdussalam et al.[26] deviate with opposite trends, being that the maximum deviation between these two studies found in the literature is 0.40%.

From the comparison of the experimental data of *n*-heptane with those obtained with the Lemmon and Span's equation shown in Figure 3, it is found that the maximum deviation is 0.13% and the average absolute deviation is 0.05%. Regardless of the experimental condition, the deviation is lower than expanded uncertainties $U_c(\rho)$ calculated with the conventional coverage factor $k$ = 2, which are represented by dashed lines in Figure 3. Thus, these data agree within the entire range of temperature and pressure investigated.

Figure 4 shows the deviations obtained between the experimental densities of *n*-dodecane with those found in the literature. In comparison to the data reported by Valencia et al.,[31] Regueira et al.,[32] García-Morales et al.,[33] and Bazile et al.,[12] the deviations are mainly within the relative deviations of ±0.05%. However, higher deviations occur from the data reported by Landau and Würflinger,[27] Khasanshin et al.,[29] and Dzida and Cempa[3] of 0.15, 0.09, and 0.07%, respectively. It is worth mentioning that, as in this study, the density measurements by Valencia et al.[31] and Bazile et al.[12] were made with a vibrating tube densitometer. On the other hand, densities reported by Landau and Würflinger,[27] Khasanshin et al.,[29] and Dzida and Cempa[3] were obtained from other methods (see Table 4). Thus, it can be highlighted that different methods for obtaining density might lead to higher deviations.

Figure 5 shows the densities of the binary mixtures *n*-heptane (1) + *n*-dodecane (mole fraction $x_1$ = 0.1999, 0.3991, 0.5999, and 0.7998) along eight isotherms from (293.15 to 363.15) K at 10 K intervals and at pressures up to 70 MPa. These results are also presented in Table 3. In this figure, the usual trend of density with pressure and temperature can be observed, i.e., it increases with the increase of pressure along each isotherm. The correlative capability of density through the polynomial equation (Section 2.3) is also depicted in Figure 5 where calculated densities (dashed lines) are plotted along with experimental data. High-pressure liquid densities for the *n*-heptane + *n*-dodecane system were also reported by Dzida and Cempa;[3] however, these data cannot be directly compared with our results because they were measured at different compositions $x$ = (0.1014, 0.3007, 0.4999, 0.7007, 0.8499, 0.9391, 0.9700).

Table 5 gathers the fitting parameters of the polynomial and Tait equations as well as additional statistical values for each isopleth evaluated in this study. The polynomial model presented slightly lower AAD values than the Tait-based equation for each isopleth, being on average 0.011 and 0.012%,


https://dx.doi.org/10.1021/acs.jced.0c00943
J. Chem. Eng. Data 2021, 66, 1305−1318

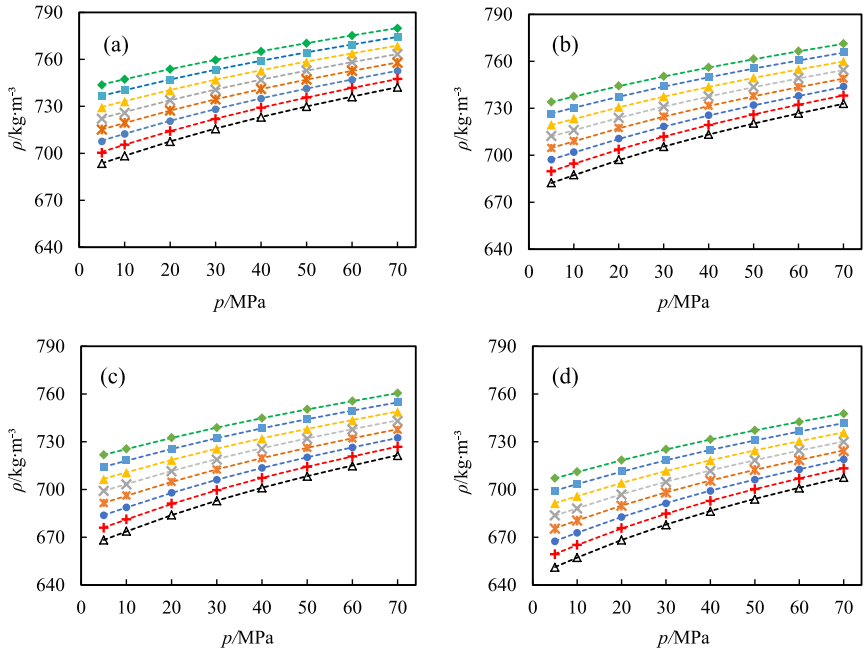


**Figure 5.** Density, $\rho$, of the *n*-heptane (1) + *n*-dodecane binary mixture in different isotherms as a function of pressure: (a) $x_1$ = 0.1999, (b) $x_1$ = 0.3991, (c) $x_1$ = 0.5999, (d) $x_1$ = 7998. (Green tilted square solid) 293.15 K, (blue box solid) 303.15 K, (yellow triangle up solid) 313.15 K, (gray multiplication sign) 323.15 K, (orange asterisk) 333.15 K, (blue circle solid) 343.15 K, (red plus sign) 353.15 K, and (Δ) 363.15 K. The dashed lines are densities calculated with the polynomial model.

**Table 5. Parameters and Deviations for Density Correlation Obtained with the Polynomial Model and Tait Equation Related to *n*-Heptane (1), *n*-Dodecane, and Their Binary Mixtures**

| parameters | $x_1$ = 0 | $x_1$ = 0.1999 | $x_1$ = 0.3991 | $x_1$ = 0.5999 | $x_1$ = 0.7998 | $x_1$ = 1 |
|---|---|---|---|---|---|---|
| Polynomial Model ($p_{ref}$ = 5 MPa, $T_{ref}$ = 293.15 K) | | | | | | |
| $10^3$ $a$/K$^{-1}$ | 1.055 | 1.418 | -0.028 | 3.421 | 1.505 | 2.863 |
| $10^5$ $b$/K$^{-2}$ | −0.182 | −0.369 | 0.488 | −1.609 | −0.444 | −1.328 |
| $10^8$ $c$/K$^{-3}$ | 0.473 | 0.731 | −0.494 | 2.738 | 1.043 | 2.563 |
| $10^3$ $a_0^P$/MPa$^{-1}$ | 4.745 | 2.891 | 3.823 | 5.790 | 6.835 | 8.473 |
| $10^{10}$ $a_1^P$/MPa$^{-2}$ | −2.543 | −1.913 | −2.072 | −2.822 | −3.318 | −3.617 |
| $10^{18}$ $a_2^P$/MPa$^{-3}$ | 3.216 | 2.832 | 2.755 | 3.457 | 3.979 | 3.868 |
| $10^5$ $b_0^P$/MPa$^{-1}$·K$^{-1}$ | −2.938 | −1.794 | −2.436 | −3.734 | −4.464 | −5.614 |
| $10^{12}$ $b_1^P$/MPa$^{-2}$·K$^{-1}$ | 1.608 | 1.215 | 1.342 | 1.842 | 2.177 | 2.410 |
| $10^{20}$ $b_2^P$/MPa$^{-3}$·K$^{-1}$ | −2.010 | −1.768 | −1.746 | −2.219 | −2.567 | −2.539 |
| $10^7$ $c_0^P$/MPa$^{-1}$·K$^{-2}$ | 0.562 | 0.394 | 0.508 | 0.731 | 0.871 | 1.088 |
| $10^{15}$ $c_1^P$/MPa$^{-2}$·K$^{-2}$ | −2.640 | −2.053 | −2.290 | −3.140 | −3.729 | −4.203 |
| $10^{23}$ $c_0^P$/MPa$^{-3}$·K$^{-2}$ | 3.185 | 2.825 | 2.824 | 3.631 | 4.229 | 4.284 |
| $\sigma$/kg·m$^{-3}$ | 0.110 | 0.123 | 0.106 | 0.112 | 0.090 | 0.148 |
| AAD/% | 0.009 | 0.012 | 0.010 | 0.011 | 0.008 | 0.014 |
| MD/% | 0.047 | 0.043 | 0.040 | 0.036 | 0.042 | 0.080 |
| Tait ($p_{ref}$ = 5 MPa) | | | | | | |
| $10^{-2}$ $A_0$/kg m$^{-3}$ | 9.545 | 9.531 | 9.273 | 9.349 | 9.127 | 8.790 |
| $A_1$/kg m$^{-3}$ K$^{-1}$ | −0.675 | −0.709 | −0.595 | −0.696 | −0.621 | −0.493 |
| $10^6$ $A_2$/kg m$^{-3}$ K$^{-2}$ | −0.478 | −0.165 | −2.189 | −1.046 | −2.718 | −5.281 |
| $10^{-2}$ $B_0$/MPa | 4.087 | 4.198 | 3.725 | 3.825 | 3.597 | 3.447 |
| $B_1$/MPa K$^{-1}$ | −1.525 | −1.652 | −1.374 | −1.487 | −1.403 | −1.358 |
| $10^3$ $B_2$/MPa K$^{-2}$ | 1.534 | 1.760 | 1.340 | 1.535 | 1.431 | 1.383 |
| $10^2$ $C$ | 8.759 | 8.617 | 8.868 | 8.805 | 8.789 | 8.965 |
| $\sigma$/kg·m$^{-3}$ | 0.108 | 0.126 | 0.110 | 0.125 | 0.094 | 0.156 |
| AAD/% | 0.010 | 0.013 | 0.011 | 0.014 | 0.009 | 0.015 |
| MD/% | 0.045 | 0.042 | 0.041 | 0.037 | 0.046 | 0.089 |

respectively. The average standard deviations of the fit ($\sigma$) are also quite similar in both models, 0.115 and 0.120 kg·m$^{-3}$, respectively. These AAD and $\sigma$ values pointed out that the two models correlate quite similarly the density values.

*3.1.2. Carbon Dioxide + n-Heptane + n-Dodecane System.* The measured densities for the $CO_2$ + *n*-heptane + *n*-dodecane ternary systems are presented in Table 6. These values are also illustrated in Figure 6 as a function of pressure



https://dx.doi.org/10.1021/acs.jced.0c00943
J. Chem. Eng. Data 2021, 66, 1305−1318

**Table 6. Experimental Densities, $\rho$/kg·m$^{-3}$, for $CO_2$ (1) + *n*-Heptane (2) + *n*-Dodecane Ternary Mixture at Temperature *T*, Pressure *p*, and Composition $x_2 = x_3 = (1 - x_1)/2$**

| *p*/MPa | *T*/K | $x_1$ = 0.4904 | *T*/K | $x_1$ = 0.4904 |
|---|---|---|---|---|
| 5 | 293.15 | 761.7 | | |
| 10 | 293.15 | 768.0 | 333.15 | 723.8 |
| 20 | 293.15 | 778.9 | 333.15 | 738.4 |
| 30 | 293.15 | 788.4 | 333.15 | 750.6 |
| 40 | 293.15 | 797.0 | 333.15 | 761.3 |
| 50 | 293.15 | 804.7 | 333.15 | 770.9 |
| 60 | 293.15 | 812.0 | 333.15 | 779.3 |
| 70 | 293.15 | 818.7 | 333.15 | 787.1 |
| 5 | 303.15 | 750.0 | | |
| 10 | 303.15 | 756.5 | 343.15 | 712.6 |
| 20 | 303.15 | 768.2 | 343.15 | 728.3 |
| 30 | 303.15 | 778.4 | 343.15 | 741.4 |
| 40 | 303.15 | 787.4 | 343.15 | 752.8 |
| 50 | 303.15 | 795.6 | 343.15 | 762.8 |
| 60 | 303.15 | 803.1 | 343.15 | 771.7 |
| 70 | 303.15 | 810.1 | 343.15 | 780.1 |
| 5 | 313.15 | 738.7 | | |
| 10 | 313.15 | 745.8 | 353.15 | 701.1 |
| 20 | 313.15 | 758.3 | 353.15 | 718.3 |
| 30 | 313.15 | 769.1 | 353.15 | 732.3 |
| 40 | 313.15 | 778.8 | 353.15 | 744.3 |
| 50 | 313.15 | 787.4 | 353.15 | 754.8 |
| 60 | 313.15 | 795.2 | 353.15 | 764.1 |
| 70 | 313.15 | 802.4 | 353.15 | 772.8 |
| 10 | 323.15 | 734.6 | 363.15 | 689.3 |
| 20 | 323.15 | 748.2 | 363.15 | 708.0 |
| 30 | 323.15 | 759.7 | 363.15 | 722.8 |
| 40 | 323.15 | 769.8 | 363.15 | 735.6 |
| 50 | 323.15 | 779.2 | 363.15 | 746.6 |
| 60 | 323.15 | 787.5 | 363.15 | 756.3 |
| 70 | 323.15 | 795.1 | 363.15 | 765.3 |
| *p*/MPa | *T*/K | $x_1$ = 0.7425 | *T*/K | $x_1$ = 0.7425 |
| 5 | 293.15 | 793.3 | | |
| 10 | 293.15 | 804.6 | 333.15 | 731.0 |
| 20 | 293.15 | 823.1 | 333.15 | 761.1 |
| 30 | 293.15 | 838.2 | 333.15 | 782.7 |
| 40 | 293.15 | 851.3 | 333.15 | 800.4 |
| 50 | 293.15 | 862.8 | 333.15 | 815.1 |
| 60 | 293.15 | 873.3 | 333.15 | 828.1 |
| 70 | 293.15 | 882.7 | 333.15 | 839.4 |
| 10 | 303.15 | 787.2 | 343.15 | |
| 20 | 303.15 | 808.0 | 343.15 | 744.8 |
| 30 | 303.15 | 824.6 | 343.15 | 768.6 |
| 40 | 303.15 | 838.6 | 343.15 | 787.6 |
| 50 | 303.15 | 851.0 | 343.15 | 803.2 |
| 60 | 303.15 | 862.0 | 343.15 | 816.9 |
| 70 | 303.15 | 871.9 | 343.15 | 829.1 |
| 10 | 313.15 | 769.2 | 353.15 | |
| 20 | 313.15 | 792.3 | 353.15 | 728.3 |
| 30 | 313.15 | 810.3 | 353.15 | 754.5 |
| 40 | 313.15 | 826.0 | 353.15 | 774.7 |
| 50 | 313.15 | 839.2 | 353.15 | 791.5 |
| 60 | 313.15 | 850.8 | 353.15 | 805.9 |
| 70 | 313.15 | 861.3 | 353.15 | 818.3 |
| 10 | 323.15 | 750.5 | 363.15 | |
| 20 | 323.15 | 776.8 | 363.15 | 711.1 |
| 30 | 323.15 | 796.5 | 363.15 | 739.7 |
| 40 | 323.15 | 812.9 | 363.15 | 761.8 |
| 50 | 323.15 | 826.9 | 363.15 | 779.9 |
| 60 | 323.15 | 839.2 | 363.15 | 794.9 |
| 70 | 323.15 | 850.0 | 363.15 | 808.4 |

[a]Standard uncertainties are $u(T)$ = 0.02 K, $u(p)$ = 0.35 MPa. See Table 2 for composition uncertainty. The combined expanded uncertainty is $U_c(\rho) = 0.002 \cdot \rho$ with a 0.95 level of confidence ($k$ = 2).

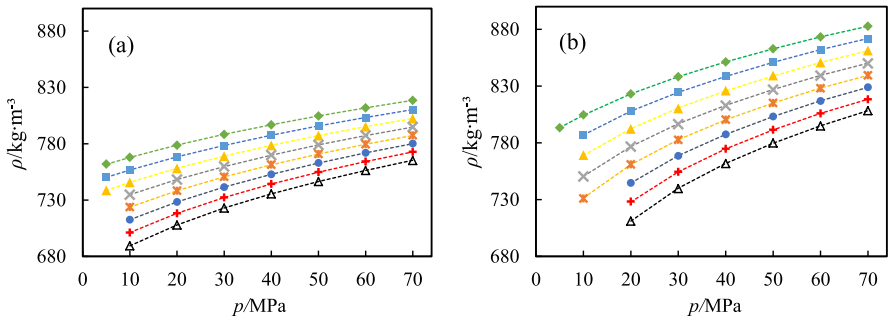


**Figure 6.** Density, $\rho$, of the $CO_2$ (1) + *n*-heptane (2) + *n*-dodecane ternary mixture in different isotherms as a function of pressure. (Green tilted square solid) 293.15 K, (blue box solid) 303.15 K, (yellow triangle up solid) 313.15 K, (gray multiplication sign) 323.15 K, (orange asterisk sign) 333.15 K, (blue circle solid) 343.15 K, (red plus sign) 353.15 K, and (Δ) 363.15 K. (a) $x_1$ = 0.4904, $x_2 = x_3$ = 0.2548, and (b) $x_1$ = 0.7425, $x_2 = x_3$ = 0.12875. The dashed lines are densities calculated with polynomial equation.

for different isotherms. The density calculated through the polynomial model (Section 2.3) is also shown in Figure 6 (dashed lines). This figure shows that the usual trend of density with pressure and temperature can be observed, i.e., it increases with the increase of pressure along each isotherm; the opposite occurs for temperature changes, i.e., density decreases if the temperature is higher.

The parameters of polynomial and Tait equations as well as the additional statistical values for each isopleth are summarized in Table 7. The Tait equation was extended to permit accurate prediction of compressed densities of ternary systems. Thus, it is important to note that it was necessary to introduce an additional fitting parameter ($A_3$) in this equation to suitably correlate the density of the mixtures with dissolved $CO_2$. In addition, the reference data used to adjust the


https://dx.doi.org/10.1021/acs.jced.0c00943
J. Chem. Eng. Data 2021, 66, 1305−1318

**Table 7. Parameters and Deviations for Density Correlation Obtained with the Polynomial Model and Tait Equation Related to $CO_2$ (1) + *n*-Heptane (2) + *n*-Dodecane Ternary Mixtures**

| parameters | $x_1$ = 0.4904, $x_2$ = $x_3$ = 0.2548 | $x_1$ = 0.7425, $x_2$ = $x_3$ = 0.12875 |
|---|---|---|
| | Polynomial Model ($p_{ref}$ = 5 MPa, $T_{ref}$ = 293.15 K) | |
| $10^3$ $a$/K$^{-1}$ | 7.608 | −1.934 |
| $10^5$ $b$/K$^{-2}$ | −4.159 | 1.693 |
| $10^8$ $c$/K$^{-3}$ | 7.105 | −0.819 |
| $10^3$ $a_0^P$/MPa$^{-1}$ | 13.778 | 5.625 |
| $10^{10}$ $a_1^P$/MPa$^{-2}$ | −5.514 | 0.376 |
| $10^{18}$ $a_2^P$/MPa$^{-3}$ | 5.594 | −1.625 |
| $10^5$ $b_0^P$/MPa$^{-1}$·K$^{-1}$ | −9.443 | −6.503 |
| $10^{12}$ $b_1^P$/MPa$^{-2}$·K$^{-1}$ | 3.742 | 0.664 |
| $10^{20}$ $b_2^P$/MPa$^{-3}$·K$^{-1}$ | −3.730 | 0.354 |
| $10^7$ $c_0^P$/MPa$^{-1}$·K$^{-2}$ | 1.823 | 1.928 |
| $10^{15}$ $c_1^P$/MPa$^{-2}$·K$^{-2}$ | −6.644 | −3.428 |
| $10^{23}$ $c_2^P$/MPa$^{-3}$·K$^{-2}$ | 6.416 | 1.251 |
| $\sigma$/kg·m$^{-3}$ | 0.164 | 0.424 |
| AAD/% | 0.016 | 0.038 |
| MD/% | 0.050 | 0.173 |
| Extended Tait | $p_{ref}$ = 10 MPa | $p_{ref}$ = 20 MPa |
| $10^{-3}$ $A_0$/kg m$^{-3}$ | 1.678 | 1.222 |
| $A_1$/kg m$^{-3}$ K$^{-1}$ | −6.659 | −1.472 |
| $10^2$ $A_2$/kg m$^{-3}$ K$^{-2}$ | 1.751 | 0.120 |
| $10^5$ $A_3$/kg m$^{-3}$ K$^{-3}$ | −1.837 | −0.282 |
| $10^{-2}$ $B_0$/MPa | 3.179 | 3.120 |
| $B_1$/MPa K$^{-1}$ | −1.321 | −1.459 |
| $10^3$ $B_2$/MPa K$^{-2}$ | 1.366 | 1.640 |
| $10^2$ $C$ | 8.761 | 9.144 |
| $\sigma$/kg·m$^{-3}$ | 0.138 | 0.217 |
| AAD/% | 0.013 | 0.020 |
| MD/% | 0.040 | 0.073 |

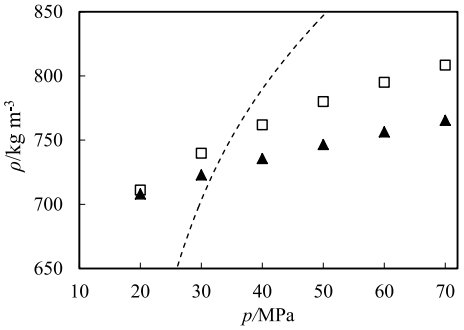


**Figure 7.** Density, $\rho$, as a function of pressure for two different isopleths at 363.15 K of the $CO_2$ (1) + *n*-heptane (2) + *n*-dodecane ternary mixtures. (▲) $x_1$ = 0.4904, $x_2$ = $x_3$ = 0.2548, (□) $x_1$ = 0.7425, $x_2$ = $x_3$ = 0.12875, and (- - -) density of pure $CO_2$ calculated by EoS of Span and Wagner[36] at 363.15 K.

parameters in eq 13 were set to values higher than the saturation pressures of each isopleth at the highest temperature. Thus, for the system with the lowest $CO_2$ content, the reference pressure is 10 MPa, and for the system with the highest $CO_2$ content, it is 20 MPa. As can be seen in Table 7, although both models present low deviations from experimental data, the extended Tait equation presented lower deviations than the polynomial model, especially for the mixture with a higher $CO_2$ concentration.

A crossover effect, the crossing of the isopleths in the ($p$,$\rho$) graph, is observed for ternary mixtures at 363.15 K and 20 MPa (Figure 7). This effect can be attributed to the density of the pure components, where the density of carbon dioxide is lower than those of linear alkanes at low pressures. At higher $CO_2$ concentrations, the mixture behavior tends to approach that of $CO_2$ and the slope of the mixture density versus pressure is steeper, causing the crossover phenomenon to appear.

Medina-Bermúdez et al.[8] and Bazile et al.[9] reported this effect for the $CO_2$ + *n*-heptane mixtures. Zhang et al.[10] and Bazile et al.[12] also reported the crossover effect for the $CO_2$ + *n*-dodecane system. In all of these studies, the crossover phenomenon was observed around 10 MPa for mixtures with a high $CO_2$ content (typically higher than 70 mol %). Medina-Bermúdez et al.[8] and Bazile et al.[9,12] only reported this effect at 313 K. However, Zhang et al.[10] reported the $CO_2$ crossover effect at (313.55, 323.55, 333.55, and 353.55) K, and from this study, it was possible to note that it is also dependent on temperature. Therefore, as can be seen in Figure 7, the crossover phenomenon in the ternary mixtures tends to occur at higher pressures and temperatures than those reported for binary systems.

**3.2. Excess Volume.** To obtain the values of the excess volumes ($V^E$, eq 21), density data of all systems are required in different compositions and at different temperatures and pressures. These values were obtained experimentally in this work (Tables 3 and 4). To calculate $V^E$ for ternary mixtures, densities of pure $CO_2$ were obtained from the EoS proposed by Span and Wagner.[36]

$$V^E(T, P) = \frac{\sum_{i=1}^{n} x_i M_i}{\rho_{mix}(T, P)} - \sum_{i=1}^{n} \left( x_i \frac{M_i}{\rho_i(T, P)} \right) \quad (21)$$



https://dx.doi.org/10.1021/acs.jced.0c00943
J. Chem. Eng. Data 2021, 66, 1305−1318

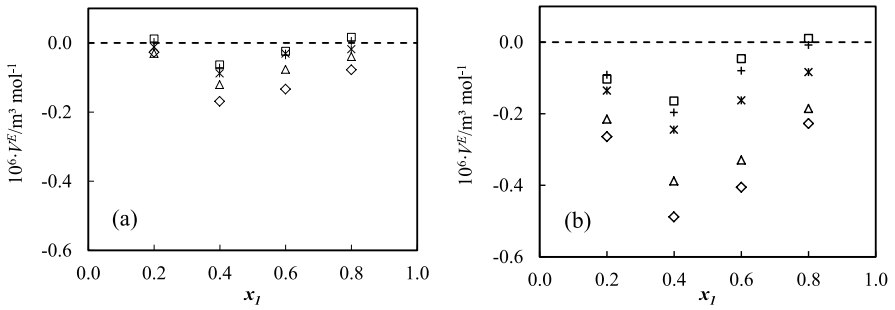


**Figure 8.** Plot of excess volume ($V^E$) against mole fraction for *n*-heptane (1) + *n*-dodecane mixtures at (a) $T$ = 293.15 K and (b) $T$ = 363.15 K: (◊) 5, (Δ) 10, (*) 30, (+) 50, (□) 70 MPa.

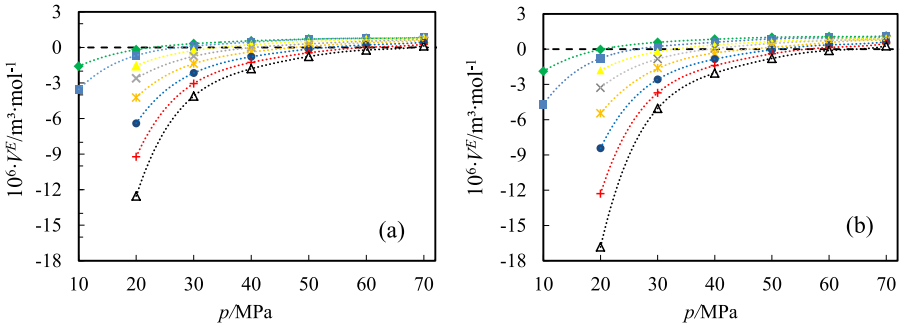


**Figure 9.** Excess volumes ($V^E$) of the $CO_2$ (1) + *n*-heptane (2) + *n*-dodecane ternary mixture in different isotherms as a function of pressure. (Green tilted square solid) 293.15 K, (blue box solid) 303.15 K, (yellow triangle up solid) 313.15 K, (gray multiplication sign) 323.15 K, (orange asterisk sign) 333.15 K, (blue circle solid) 343.15 K, (red plus sign) 353.15 K, and (Δ) 363.15 K. (a) $x_1$ = 0.4904, $x_2 = x_3$ = 0.2548, and (b) $x_1$ = 0.7425, $x_2 = x_3$ = 0.12875.

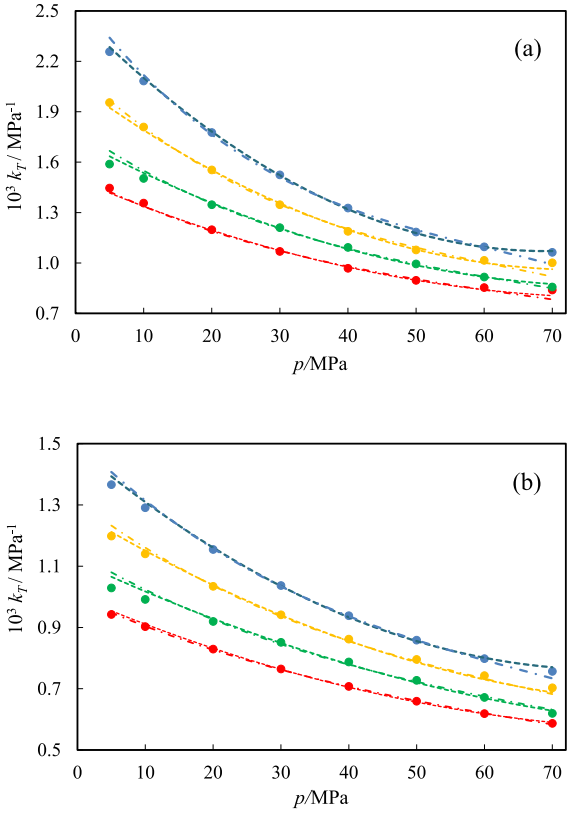


**Figure 10.** Isothermal compressibility coefficient, $k_T$, of the (a) pure *n*-heptane and (b) pure *n*-dodecane. (●) Reference data, (···) polynomial model, and (-·-) Tait. (Red) 303.15 K, (green) 323.15 K, (yellow) 343.15 K, and (blue) 363.15 K.

The excess molar volumes of *n*-heptane + *n*-dodecane mixtures are shown in Figure 8 at the lowest and highest temperatures (293.15 and 363.15) K at different pressures. The $V^E$ values increase with increasing temperature and decrease with increasing pressure. They are mostly negative over the whole concentration range but become small positive values in the heptane-rich region. It is commonly assumed that the negative $V^E$ results mainly from the free-volume effects caused by the interstitial accommodation of the shorter alkane molecules in the structure of the longer chain alkanes, which leads to a more compact and less compressible system. The increasing pressure leads to a decrease of the mean intermolecular distances causing the repulsive forces to become predominant. Consequently, this leads to a positive volume of mixing. These results agree with those of Dzida and Cempa,[3] who also reported positive $V^E$ for *n*-heptane + *n*-dodecane mixtures in the heptane-rich region at pressures from 60 to 100 MPa.

The excess molar volumes of $CO_2$ + *n*-heptane + *n*-dodecane mixtures are shown in Figure 9 as a function of pressure for the eight isotherms evaluated in this study. All of the $V^E$ values were found to be positive at the highest pressure, and their values become more negative as the pressure decreases and the temperature increases. It is worth noting that a large negative contribution to $V^E$ can result from the condensation of gas or supercritical $CO_2$ into liquid *n*-heptane + *n*-dodecane mixtures. The magnitude of this contribution depends on the extent of the gaslike behavior of the supercritical $CO_2$, which becomes more important when pressure decreases and temperature increases. Due to these effects, the minimum pressures of the $V^E$ calculations for ternary mixtures are defined in pressure and temperature values in which $CO_2$ approaches the liquidlike behavior. These points are shown in Figure 9.



https://dx.doi.org/10.1021/acs.jced.0c00943
J. Chem. Eng. Data 2021, 66, 1305−1318

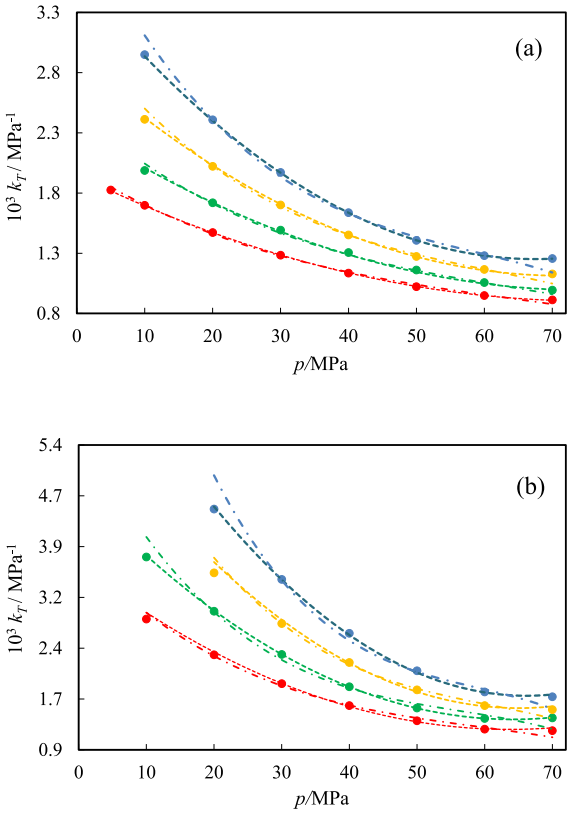


**Figure 11.** Isothermal compressibility coefficient, $k_T$, of the $CO_2$ (1) + *n*-heptane (2) + *n*-dodecane ternary mixture. (a) $x_1$ = 0.4904, $x_2$ = $x_3$ = 0.2548, and (b) $x_1$ = 0.7425, $x_2$ = $x_3$ = 0.12875. (●) Reference data, (···) polynomial model, and (---) Tait. (Red) 303.15 K, (green) 323.15 K, (yellow) 343.15 K, and (blue) 363.15 K.

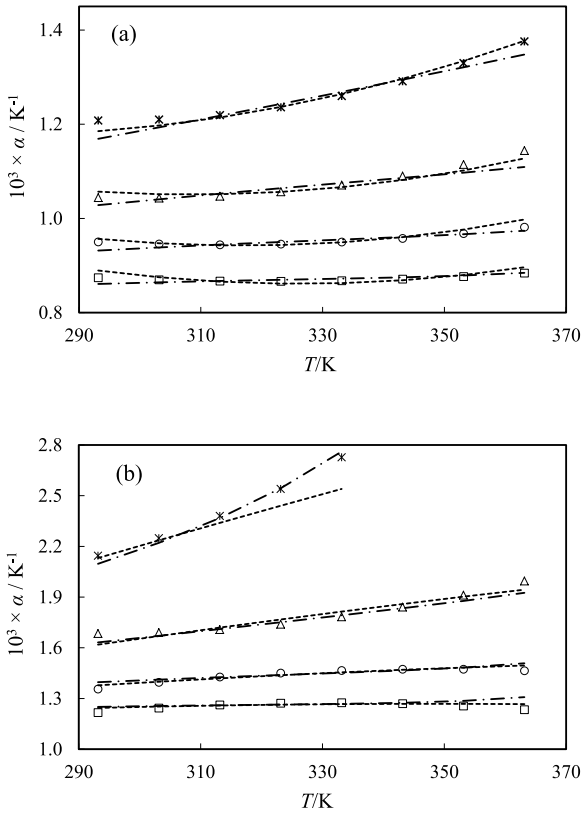


**Figure 12.** Thermal expansion coefficient, $\alpha$, of the (a) pure *n*-heptane and (b) $CO_2$ (1) + *n*-heptane (2) + *n*-dodecane ternary mixture ($x_1$ = 0.7425, $x_2$ = $x_3$ = 0.12875). (Symbols) Reference data, (···) polynomial model, and (---) Tait. (*) 10 MPa, (Δ) 30 MPa, (○) 50 MPa, and (□) 70 MPa.

**3.3. Isothermal Compressibility and Thermal Expansion Coefficients.** Numerical $k_T$ obtained according to eq 2, which is adopted as reference data, and calculated $k_T$ obtained by the models are plotted in Figures 10 and 11 at selected temperatures as a function of pressure for different studied systems. The expected trend of this property with pressure and temperature was found, that is, it decreases with an increase of pressure along the isotherms and increases with increasing temperature. The ternary system with the lowest $CO_2$ content presented, as expected, lower compressibility than the system with the highest $CO_2$ content.

Typical results of the thermal expansion coefficient as a function of temperature obtained in this study are given in Figure 12 at selected pressures for two different systems studied. In general, the $\alpha$ values follow similar behavior of $k_T$, that is, decrease with increasing pressure and increase with increasing temperature under isobaric conditions, particularly for ternary mixtures. For *n*-heptane (as for *n*-dodecane and its binary mixtures), at pressures higher than 50 MPa, a small decrease of $\alpha$ with temperature was remarked. In addition, the ternary mixture comprising *n*-heptane and *n*-dodecane with dissolved $CO_2$ at near-$CO_2$ critical pressure (10 MPa) presented a marked variation in the expansion coefficient.

For comparing the numerical derivative properties with those obtained with the correlations presented in Section 2.3, the absolute average deviation (AAD), the maximum deviation (MD), and the standard deviation ($\sigma$) are calculated according to eqs 18−20, respectively. The results are presented in Tables 8 and 9.

Although both models presented quite low deviations from experimental density, the analysis of derivative properties shows significant differences in the quality of correlations. For instance, from Table 8, it is possible to note that the isothermal compressibility coefficient obtained from the reference model (numerical $k_T$) is better described by the polynomial model than by the Tait model for all systems evaluated in this study. The deviations shown by the Tait model increase with increasing temperature (as seen in Figures 10 and 11). On the other hand, the polynomial model represented quite well the reference data regardless of temperature and pressure variation.

Table 9 shows that the numerical $\alpha$ is better described by the polynomial model than by the Tait model for *n*-heptane/*n*-dodecane systems. For these systems, the Tait model leads to high deviations at the ends of the isobars mainly at low pressures (as seen in Figure 12a). This effect was not found for the polynomial model, which represented quite well this property. For ternary mixtures containing dissolved $CO_2$, the extended Tait and polynomial models presented quite similar performances (as seen from the AAD% values). However, it can also be seen in Figure 12b that the extended Tait performed better than the polynomial model in the vicinity of critical $CO_2$ conditions.

## 4. CONCLUSIONS

New experimental density data for the *n*-heptane + *n*-dodecane binary mixture and the ternary mixture comprising *n*-heptane and *n*-dodecane with dissolved $CO_2$ have been provided over wide temperature and pressure ranges. Density values for pure


https://dx.doi.org/10.1021/acs.jced.0c00943
J. Chem. Eng. Data 2021, 66, 1305−1318

Table 8. Deviations for Isothermal Compressibility Coefficient, $k_T$, Using Equations 18−20

| | $x_1 = 0$ | $x_1 = 0.2$ | $x_1 = 0.4$ | $x_1 = 0.6$ | $x_1 = 0.8$ | $x_1 = 1$ | $x_{CO_2} = 0.5$ | $x_{CO_2} = 0.75$ |
|---|---|---|---|---|---|---|---|---|
| | | | | Polynomial | | | | |
| $10^5\ \sigma/MPa^{-1}$ | 1.36 | 2.08 | 1.10 | 1.30 | 1.32 | 1.86 | 0.93 | 5.85 |
| AAD/% | 0.88 | 1.21 | 0.65 | 0.75 | 0.73 | 1.04 | 0.43 | 1.41 |
| MD/% | 3.57 | 7.06 | 3.59 | 3.29 | 3.59 | 5.82 | 2.22 | 5.06 |
| | | | | Tait | | | | Extended Tait |
| $10^5\ \sigma/MPa^{-1}$ | 1.56 | 2.25 | 1.57 | 1.80 | 2.18 | 2.96 | 4.48 | 15.33 |
| AAD/% | 1.13 | 1.64 | 1.01 | 1.07 | 1.21 | 1.64 | 1.80 | 3.72 |
| MD/% | 5.03 | 6.33 | 4.94 | 5.35 | 6.51 | 8.39 | 8.94 | 14.68 |

Table 9. Deviations for Thermal Expansion Coefficient, $\alpha$, Using Equations 18−20

| | $x_1 = 0$ | $x_1 = 0.2$ | $x_1 = 0.4$ | $x_1 = 0.6$ | $x_1 = 0.8$ | $x_1 = 1$ | $x_{CO_2} = 0.5$ | $x_{CO_2} = 0.75$ |
|---|---|---|---|---|---|---|---|---|
| | | | | Polynomial | | | | |
| $10^5\ \sigma/K^{-1}$ | 1.44 | 2.04 | 0.64 | 0.60 | 0.54 | 1.50 | 1.35 | 4.65 |
| AAD/% | 1.24 | 1.29 | 0.41 | 0.42 | 0.37 | 0.83 | 0.49 | 1.23 |
| MD/% | 3.61 | 6.44 | 2.71 | 1.68 | 1.34 | 5.28 | 3.35 | 6.93 |
| | | | | Tait | | | | Extended Tait |
| $10^5\ \sigma/K^{-1}$ | 1.48 | 1.93 | 0.82 | 1.57 | 0.86 | 2.01 | 1.18 | 2.80 |
| AAD/% | 1.32 | 1.43 | 0.57 | 1.25 | 0.63 | 1.10 | 0.46 | 1.15 |
| MD/% | 4.29 | 6.24 | 3.34 | 5.22 | 2.33 | 7.63 | 4.21 | 5.99 |

*n*-heptane and *n*-dodecane were found to be in agreement with literature data within approximately 0.3%. All experimental data were well correlated using Amorim's polynomial model and a Tait-based model. The excess molar volume was calculated for whole ranges of temperature, pressure, and composition. In general, the excess volumes determined in this study are negative and become positive in the heptane-rich region and at pressures above 50 MPa. For ternary mixtures, the absolute values of this property have been found to be relatively high at the lowest pressures and highest temperatures studied, which can be explained by the extension of the gaslike behavior of the pure $CO_2$ under some conditions of temperature and pressure of the experiments. The derived thermodynamic properties, that is, the thermal expansion coefficient and the isothermal compressibility coefficient, were calculated from experimental density data using both polynomial and Tait equations. The analysis of these properties pointed out that, in general, the polynomial model provided more accurate results related to the derived thermodynamic properties.

## ■ ASSOCIATED CONTENT

### Supporting Information

The Supporting Information is available free of charge at https://pubs.acs.org/doi/10.1021/acs.jced.0c00943.

A detailed description of how the estimated standard uncertainties, *u*, used in eq S2 are obtained to obtain estimated combined uncertainties for experimental densities (Table S1) (PDF)

## ■ AUTHOR INFORMATION


### Corresponding Author

**Márcio L. L. Paredes** − *Institute of Chemistry, Rio de Janeiro State University, Rio de Janeiro, RJ 20550-900, Brazil;* orcid.org/0000-0002-4623-1897; Email: paredes@uerj.br

### Authors

**David C. Santos** − *School of Chemistry and Laboratory of Enhanced Oil Recovery, Federal University of Rio de Janeiro, Rio de Janeiro, RJ 21945-970, Brazil*

**Isaque S. Gonçalves** − *School of Chemistry, Federal University of Rio de Janeiro, Rio de Janeiro, RJ 21945-970, Brazil*

**Ana Mehl** − *School of Chemistry, Federal University of Rio de Janeiro, Rio de Janeiro, RJ 21945-970, Brazil*

**Paulo Couto** − *Civil Engineering Program, COPPE, Federal University of Rio de Janeiro, Rio de Janeiro, RJ 21945-970, Brazil; Laboratory of Enhanced Oil Recovery, Federal University of Rio de Janeiro, Rio de Janeiro, RJ 21941-594, Brazil*

Complete contact information is available at: https://pubs.acs.org/10.1021/acs.jced.0c00943


### Notes

The authors declare no competing financial interest.

## ■ ACKNOWLEDGMENTS

This research was carried out in association with the ongoing R&D project registered as ANP no 20352−1, "Caracterização de Fluidos Complexos em Condições de Reservatórios de Petróleo Brasileiros" (UFRJ/Shell Brasil/ANP), sponsored by Shell Brazil under the ANP R&D levy as "Compromisso de Investimentos com Pesquisa e Desenvolvimento".

## ■ REFERENCES

(1) Rezk, M. G.; Foroozesh, J. Effect of $CO_2$ mass transfer on rate of oil properties changes: Application to $CO_2$-EOR projects. *J. Pet. Sci. Eng.* **2019**, *180*, 298−309.

(2) Hawthorne, S. B.; Grabanski, C. B.; Miller, D. J.; Kurz, B. A.; Sorensen, J. A. Hydrocarbon recovery from Williston Basin Shale and mudrock cores with supercritical $CO_2$: 2. Mechanisms that control oil recovery rates and $CO_2$ permeation. *Energy Fuels* **2019**, *33*, 6867−6877.

(3) Dzida, M.; Cempa, M. Thermodynamic and acoustic properties of (heptane + dodecane) mixtures under elevated pressures. *J. Chem. Thermodyn.* **2008**, *40*, 1531−1541.

(4) Fenghour, A.; Trusler, J. P. M.; Wakeham, W. A. Densities and bubble points of binary mixtures of carbon dioxide and n-heptane and ternary mixtures of n-butane, n-heptane and n-hexadecane. *Fluid Phase Equilib.* **2001**, *185*, 349−358.
(5) Al Ghafri, S. Z.; Maitland, G. C.; Trusler, J. P. M. Experimental and modeling study of the phase behavior of synthetic crude oil +$CO_2$. *Fluid Phase Equilib.* **2014**, *365*, 20−40.
(6) Chacon Valero, A. M. C.; Feitosa, F. X.; Sant'Ana, H. B. Density and volumetric behavior of binary $CO_2$ + n-decane and ternary $CO_2$ + n-decane + naphthalene systems at high pressure and high temperature. *J. Chem. Eng. Data* **2020**, *65*, 3499−3509.
(7) Cardoso, S. G.; Costa, G. M. N.; Melo, S. A. B. Assessment of the liquid mixture density effect on the prediction of supercritical carbon dioxide volume expansion of organic solvents by Peng-Robinson equation of state. *Fluid Phase Equilib.* **2016**, *425*, 196−205.
(8) Medina-Bermúdez, M.; Molina, L. A. S.; Tiburcio, W. E.; Luna, L. A. G.; Solis, O. E. (p, $\rho$, T) Behavior for the Binary Mixtures Carbon Dioxide + Heptane and Carbon Dioxide + Tridecane. *J. Chem. Eng. Data* **2013**, *58*, 1255−1264.
(9) Bazile, J. P.; Nasri, D.; Hamani, A. W. S.; Galliero, G.; Daridon, J. L. Excess volume, isothermal compressibility, isentropic compressibility and speed of sound of carbon dioxide + n-heptane binary mixture under pressure up to 70 MPa. I Experimental Measurements. *J. Supercrit. Fluids* **2018**, *140*, 218−232.
(10) Zhang, Y.; Liu, Z.; Liu, W.; Zhao, J.; Yang, M.; Liu, Y.; Wang, D.; Song, Y. Measurement and modeling of the densities for $CO_2$ + dodecane system from 313.55 K to 353.55 K and pressures up to 18 MPa. *J. Chem. Eng. Data* **2014**, *59*, 3668−3676.
(11) Zambrano, J.; Soto, F. V. G.; Martín, D. L.; Martín, M. C.; Segovia, J. J. Volumetric behaviour of (carbon dioxide + hydrocarbon) mixtures at high pressures. *J. Supercrit. Fluids* **2016**, *110*, 103−109.
(12) Bazile, J. P.; Nasri, D.; Hamani, A. W. S.; Galliero, G.; Daridon, J. L. Density, Speed of Sound, Compressibility, and excess properties of carbon dioxide + n-dodecane binary mixtures from 10 to 70 MPa. *J. Chem. Eng. Data* **2019**, *64*, 3187−3204.
(13) Amorim, J. A.; Chiavone, O.; Paredes, M. L. L.; Rajagopal, K. Modeling high-pressure densities at wide temperature range with volume scaling: Cyclohexane + n-hexadecane mixtures. *Fluid Phase Equilib.* **2007**, *259*, 89−98.
(14) Lagourette, B.; Boned, C.; Guirons, H.; Xans, P.; Zhou, H. Densimeter calibration method versus temperature and pressure. *Meas. Sci. Technol.* **1992**, *3*, 699−703.
(15) Comuñas, M. J.; Bazile, J. P.; Baylaucq, A.; Boned, C. Density of diethyl adipate using a new vibrating tube densimeter from (293.15 to 403.15) K and up to 140 MPa. Calibration and Measurements. *J. Chem. Eng. Data* **2008**, *53*, 986−994.
(16) Wagner, W.; Pruß, A. The IAPWS formulation 1995 for the thermodynamic properties of ordinary water substance for general and scientific use. *J. Phys. Chem. Ref. Data* **2002**, *31*, 387−535.
(17) Al Motari, M. M.; Kandil, M. E.; Marsh, K. N.; Goodwin, A. R. H. Density and viscosity of diisodecyl phthalate $C_6H_4(COOC_{10}H_{21})_2$, with nominal viscosity at T = 298 K, and p = 0.1 MPa of 87 mPa·s, at temperatures from (298.15 to 423.15) K and pressures up to 70 MPa. *J. Chem. Eng. Data* **2007**, *52*, 1233−1239.
(18) Caudwell, D. R.; Trusler, J. P. M.; Vesovic, V.; Wakeham, W. A. The Viscosity and Density of n-Dodecane and n-Octadecane at Pressures up to 200 MPa and Temperatures up to 473 K. *Int. J. Thermophys.* **2004**, *25*, 1339−1352.
(19) Holcomb, C. D.; Outcalt, S. L. A theoretically-based calibration and evaluation procedure for vibrating-tube densimeters. *Fluid Phase Equilib.* **1998**, *150−151*, 815−827.
(20) Chirico, R. D.; Frenkel, M.; Magee, J. W.; Diky, V.; Muzny, C. D.; Kazakov, A. F.; Kroenlein, K.; Abdulagatov, I.; Hardin, G. R.; Acree, W. E.; Brenneke, J. F.; Brown, P. L.; Cummings, P. T.; Loos, T. W.; Friend, D. G.; Goodwin, A. R. H.; Hansen, L. D.; Haynes, W. M.; Koga, N.; Mandelis, A.; Marsh, K. N.; Mathias, P. M.; McCabe, C.; O'Connell, J. P.; Padua, A.; Rives, V.; Schick, C.; Trusler, J. P. M.; Vyazovkin, S.; Weir, R. D.; Wu, J. Improvement of quality in publication of experimental thermophysical property data: Challenges, assessment tools, global implementation, and online support. *J. Chem. Eng. Data* **2013**, *58*, 2699−2716.
(21) Peng, R. Y.; Robinson, D. B. A new two constant equation of state. *Ind. Eng. Chem. Fundam.* **1976**, *15*, 59−64.
(22) Lagarias, J. C.; Reeds, J. A.; Wright, M. H.; Wright, P. E. Convergence properties of the Nelder-Mead simplex method in low dimensions. *SIAM J. Optim.* **1998**, *9*, 112−147.
(23) Dymond, J. H.; Malhotra, R. The Tait equation: 100 years on. *Int. J. Thermophys.* **1988**, *9*, 941−951.
(24) Sagdeev, D. I.; Fomina, M. G.; Mukhamedzyanov, G. K.; Abdulagatov, I. M. Experimental study of the density and viscosity of n-heptane at temperatures from 298 K to 470 K and pressure up to 245 MPa. *Int. J. Thermophys.* **2013**, *34*, 1−33.
(25) Guerrero, H.; Royo, F. M.; Gascón, I.; Lafuente, C. Excess properties from p$\rho$T data for n-heptane + isomeric chlorobutane mixtures. *Thermochim. Acta* **2015**, *614*, 100−109.
(26) Abdussalam, A. A.; Ivaniš, G. R.; Radovic, I. R.; Kijevcanin, M. L. Densities and derived thermodynamic properties for the (n-heptane + n-octane), (n-heptane + ethanol) and (n-octane + ethanol) systems at high pressures. *J. Chem. Thermodyn.* **2016**, *100*, 89−99.
(27) Landau, R.; Würflinger, A. PVT-Daten von Acetonitril, Undecan und Dodecan bis 3 kbar und −50 °C. Druckabhängigkeit der Umwandlungsvolumina, -enthalpien und -entropien. *Ber. Ges. Bunsen-Ges. Phys. Chem.* **1980**, *84*, 895−902. (In German).
(28) Dymond, J. H.; Robertson, J.; Isdale, J. D. Transport properties of nonelectrolyte liquid mixtures-III. Viscosity coefficients for n-octane, n-dodecane, and equimolar mixtures of n-octane + n-dodecane and n-hexane + n-dodecane from 25 to 100 °C at pressures up to the freezing pressure or 500 MPa. *Int. J. Thermophys.* **1981**, *2*, 133−154.
(29) Khasanshin, T. S.; Shchamialiou, A. P.; Poddubskij, O. G. Thermodynamic properties of heavy n-alkanes in the liquid state: n-dodecane. *Int. J. Thermophys.* **2003**, *24*, 1277−1289.
(30) Elizalde-Solis, O. E.; Galicia-Luna, L. A.; Camacho, L. E. High-pressure vapor−liquid equilibria for $CO_2$ + alkanol systems and densities of n-dodecane and n-tridecane. *Fluid Phase Equilib.* **2007**, *259*, 23−32.
(31) Valencia, J. L.; Salgado, D. G.; Troncoso, J.; Peleteiro, J.; Carballo, E.; Roman, L. Thermophysical characterization of liquids using precise density and isobaric heat capacity measurements as a function of pressure. *J. Chem. Eng. Data* **2009**, *54*, 904−915.
(32) Regueira, T.; Glykioti, M. L.; Stenby, E. H.; Yan, W. Densities of the Binary Systems n-Hexane + n-Decane and n-hexane + n-hexadecane up to 60 MPa and 463 K. *J. Chem. Eng. Data* **2015**, *60*, 3631−3645.
(33) García-Morales, R. G.; Solis, O. E.; Moreno, A. Z.; Bouchot, C.; Ramos, F. I. G.; Quevedo, M. G. A. Volumetric properties of 2,5-dimethylfuran in mixtures with octane or dodecane from 293 K to 393 K and pressures up to 70 MPa. *Fuel* **2017**, *209*, 299−308.
(34) Jia, T.; Bi, S.; Wu, J. Compressed liquid densities of binary mixtures of n-decane + n-dodecane at temperatures from 283 K to 363 K and pressures up to 100 MPa. *Fluid Phase Equilib.* **2018**, *459*, 65−72.
(35) Lemmon, E. W.; Span, R. Short fundamental equations of state for 20 industrial fluids. *J. Chem. Eng. Data* **2006**, *51*, 785−850.
(36) Span, R.; Wagner, W. A new equation of state for carbon dioxide covering the fluid region from the triple-point temperature to 1100 K at pressures up to 800 MPa. *J. Phys. Chem. Ref. Data* **1996**, *25*, 1509−1596.


https://dx.doi.org/10.1021/acs.jced.0c00943
*J. Chem. Eng. Data* 2021, 66, 1305−1318